Boundary layer characterization based on stability and turbulent measurements

A. Burgos-Cuevas, T. Marke, B. Pospichal, U. Löhnert, L. Pfitzenmaier | 14.11.2022

Motivation

- Instruments available in the CCRES units provide continuous measurement of temperature, humidity and velocity, which are crucial variables for monitoring Atmospheroc Boundary Layer (ABL) and better understanding the processes that determine cloud formation.
- Methodologies cappable of providing automatized monitoring of the ABL processes are crucial for ACTRIS measurements applicability.
- The homogeneous processing, that is available in ACTRIS CCRES units, can be exploided by analyzing thermal and dynamical structure and evolution in the ABL.

ACTRIS CCRES sites

- ACTRIS instruments provide a network of homogeneous data.
- Share a commun processing for Microwave Radiometer (MWR) and Wind Doppler lidars (WDL).
- **We aim to provide a synergistic product for better characterizing ABL with these two instruments.**

Velocity from WDL

Temperature from MWR

horizontal and vertical wind
in ABL and cloud base

Turbulent properties

Temperature profiles

Thermal stability

Combined synergistic product

Dynamic and stability characteristics

Universität zu Köln

Synergistic product to investigate ABL

- The structure and evolution of ABL is closely related to the formation of boundary layer clouds.
- In models, ABL height is usually estimated via Richardson bulk criteria. However, when utilizing measurements, there is no a single ABL height estimation that happens to be coincident with all methodologies.
- ACTRIS products can be crucial tools for elucidating BL processes that impact cloud formation and compare them within the network.

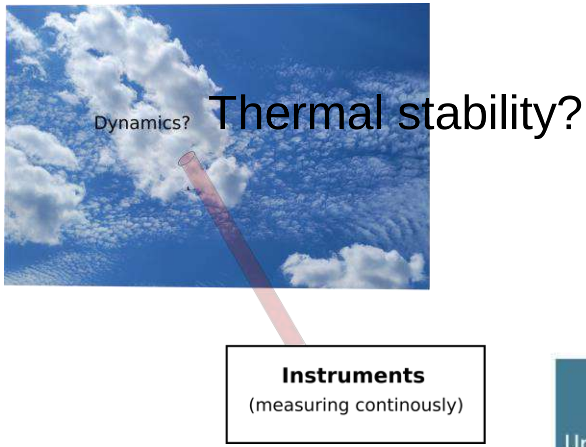

Boundary layer classification: identification of sources of turbulence

- WDL operate in CCRES units and in many Cloudnet and EARLINET sites. From their measurements, turbulence and other properties can be derived.
- Back-scatter and moments of the Doppler velocities allow to classify the turbulent mixing in the ABL (Manninen et al. 2018).

Boundary layer classification: identification of sources of turbulence

Attenuated backscatter β

Height of the aerosol layer

Cloud detection

Requires sufficient amount of aerosols as tracer for air motion

Vertical velocity skewness

Source of turbulence (surface or cloud)

$$s = \frac{\overline{w'^3}}{\overline{w'^2}^{3/2}}$$

TKE dissipation rate ε

Identify turbulent regions

Derived from vertical velocity variance (O'Connor et al., 2010)

Vector wind shear

Indicates shear driven turbulence

$$U_{shear} = \frac{\sqrt{\delta u^2 + \delta v^2}}{\delta z}$$

Boundary layer classification: identification of sources of turbulence

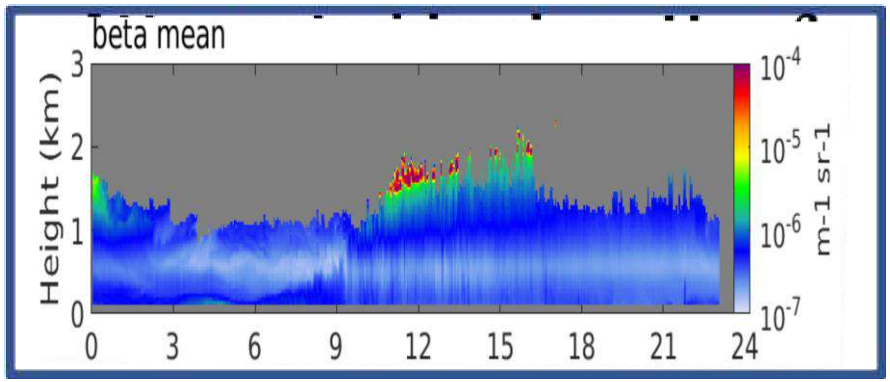

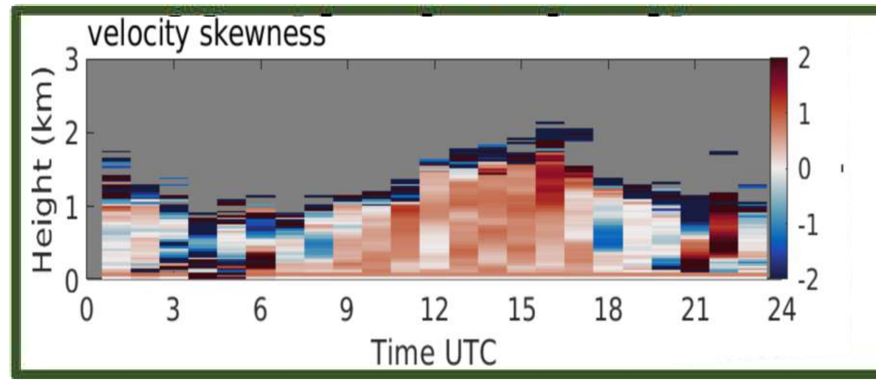

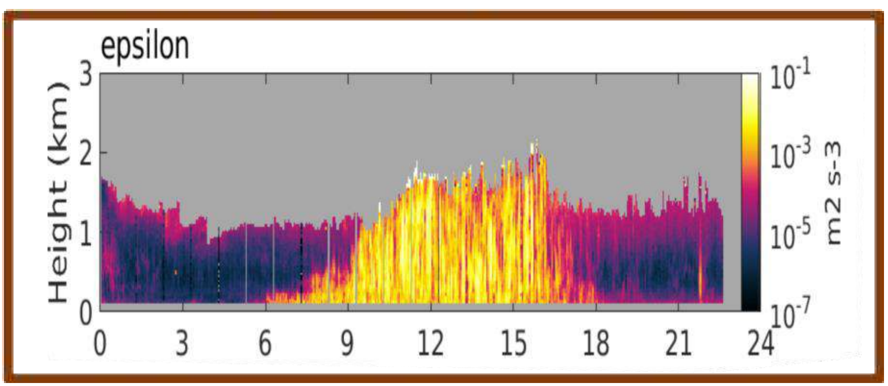

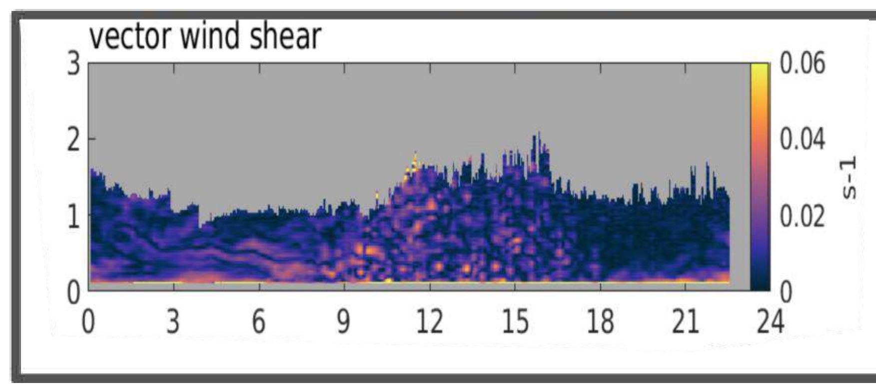

Universität zu Köln

Boundary layer classification: identification of sources of turbulence

- Identification of turbulent regions that are driven by surface fluxes or clouds.
- Better understand complex mixing processes and their evolution.

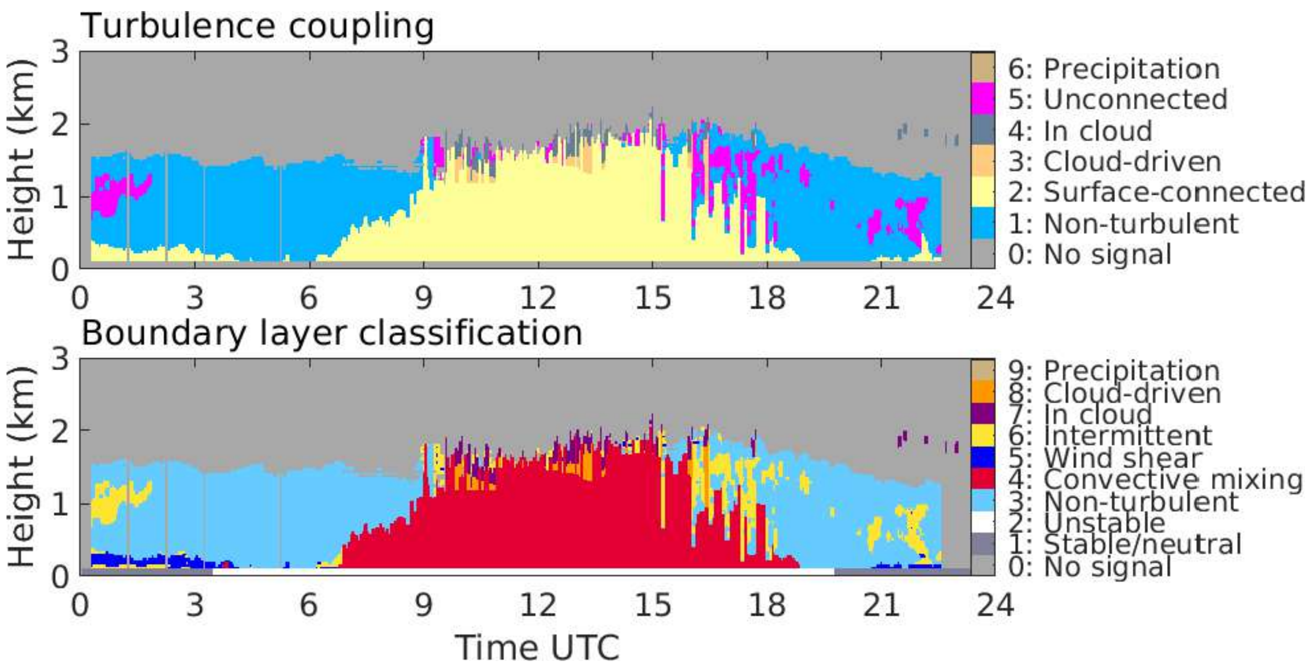

Universität zu Köln

Boundary layer thermal stability

- Temperature measurements every 50 m and with 15 min temporal resolution allows to investigate the diurnal evolution of ABL stability.
- Vertical thermal structure of the ABL investigated via **Brunt-Väisälä frequency**

$$N^2 = \frac{g}{\theta}\frac{d\theta}{dz}$$

- $N^2 > 0 \rightarrow$ *statically stable*
- $N^2 = 0 \rightarrow$ *statically neutral*
- $N^2 < 0 \rightarrow$ *statically unstable*

Boundary layer thermal stability

- Thermally stable conditions clearly visible during nighttime and instability present at daytime.

$$N^2 = \frac{g}{\theta}\frac{d\theta}{dz}$$

- $N^2 > 0 \rightarrow$ *statically stable*
- $N^2 = 0 \rightarrow$ *statically neutral*
- $N^2 < 0 \rightarrow$ *statically unstable*

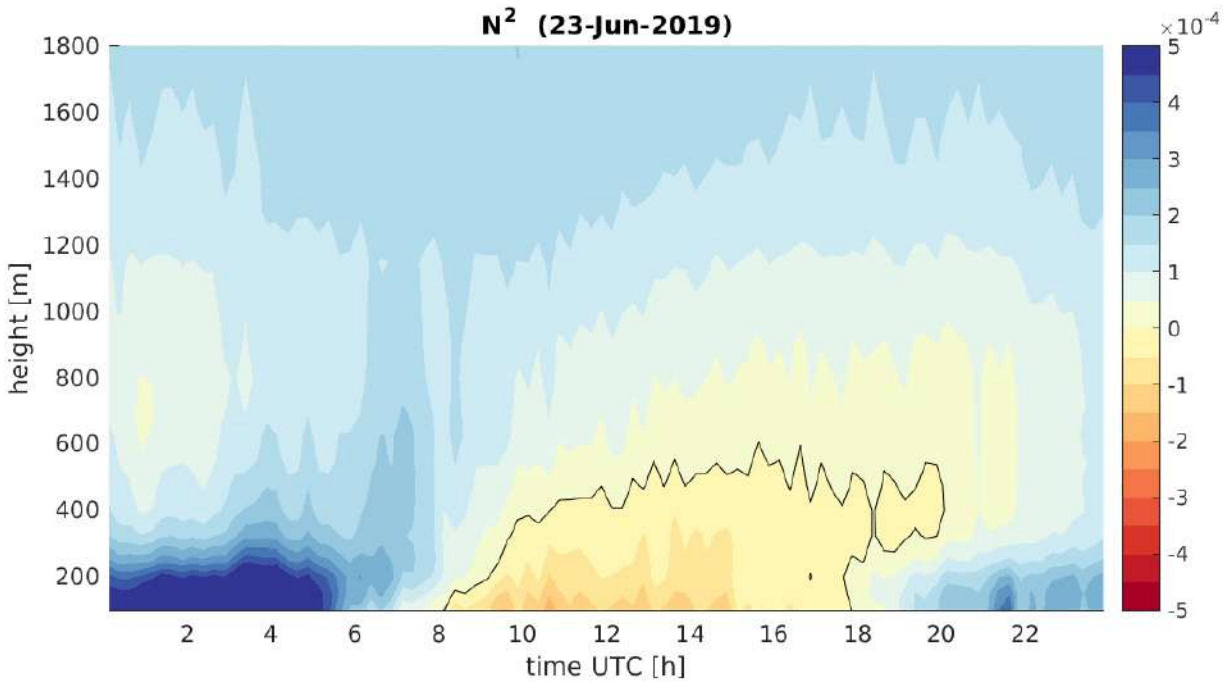

Universität zu Köln

Comparing convective layer height and N^2

- Temporal shift: convection starts shortly after 8:00 and instabilization starts later (shortly before 10:00)

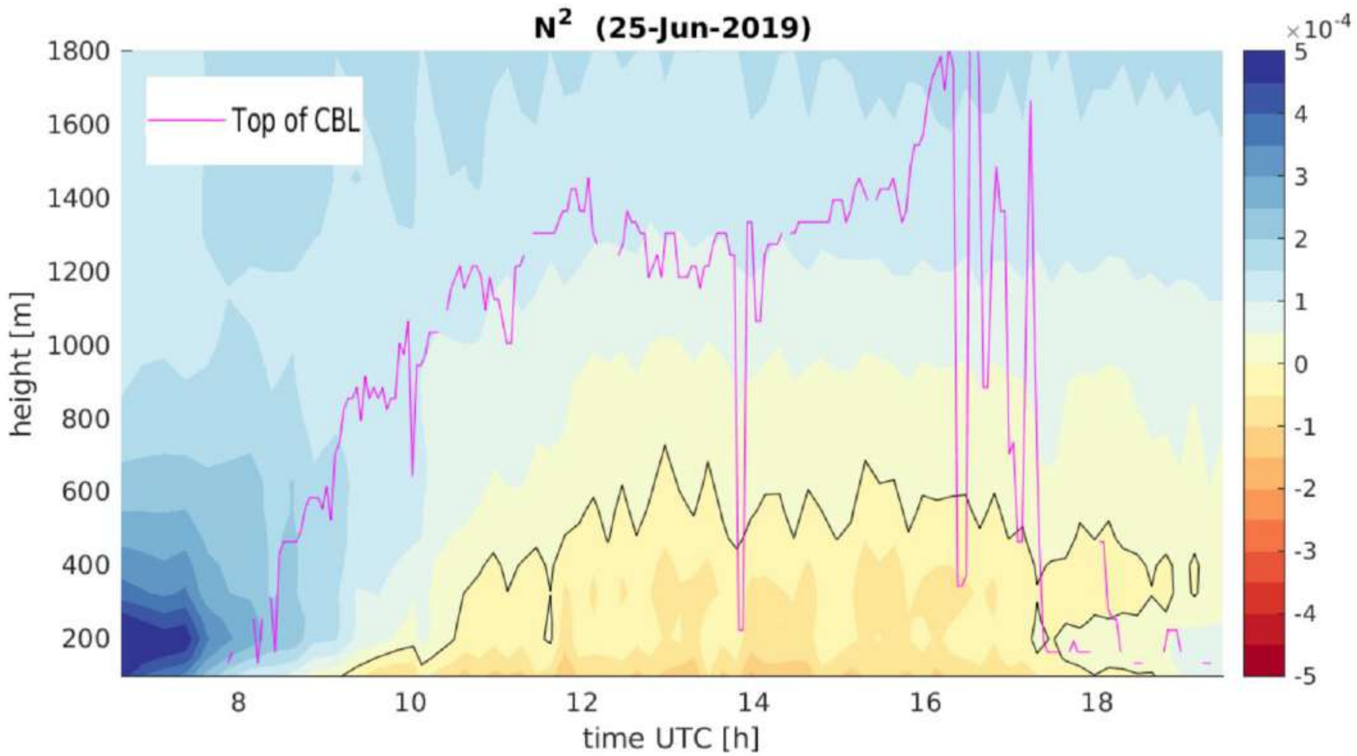

Universität zu Köln

Synergy MWR and WDL: Richardson bulk

- Relative effects of buoyancy and shear on turbulent mixing of ABL.
- ABL height estimated via Ri_B with threshold between 0.15 and 1 (0.25 most commonly used).

$$Ri_B = \frac{g}{\Theta_0} \frac{(\Theta_z - \Theta_0)z}{u^2 + v^2}$$

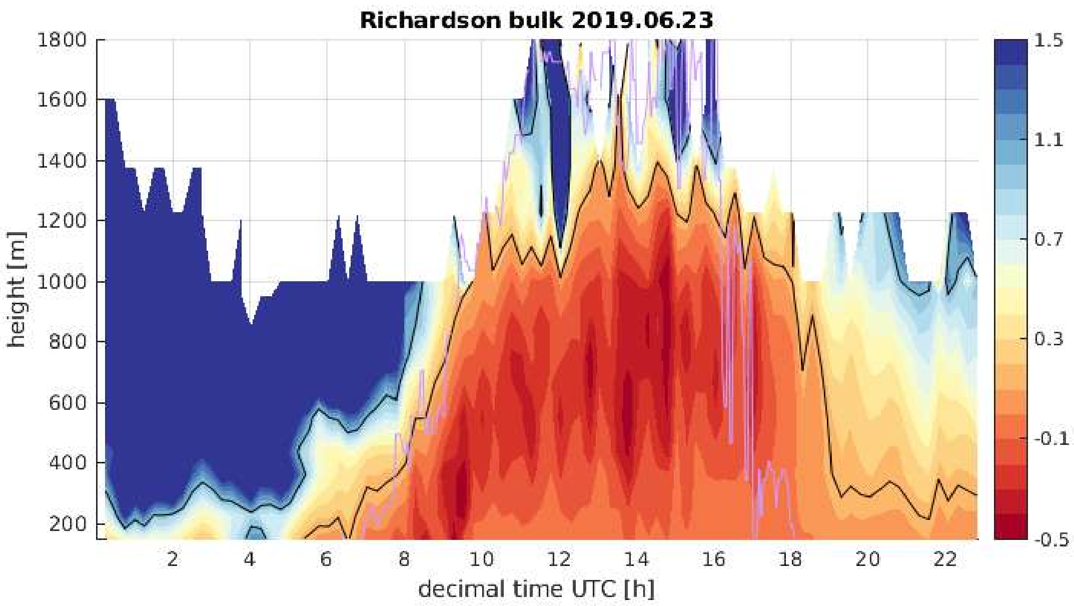

Applicability of synergistic approach in ACTRIS

- Since ACTRIS CCRES units operate MWR and WDL, synergetic products can be estimated in all of them.
- Potential to automatize this methodology in CCRES and utilize it to better characterize the ABL structure and diurnal evolution in different sites and considering both stability and dynamical processes.
- Turbulence and stability characterization can also be combined with in-situ aerosol observations in the frame of ACTRIS.

Study cases: Ri_B in summer 2019

22.06.2019

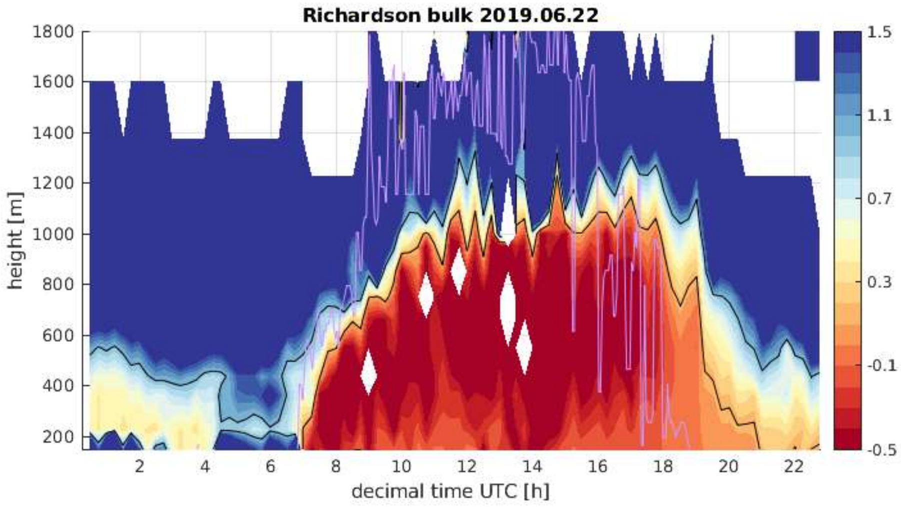

23.06.2019

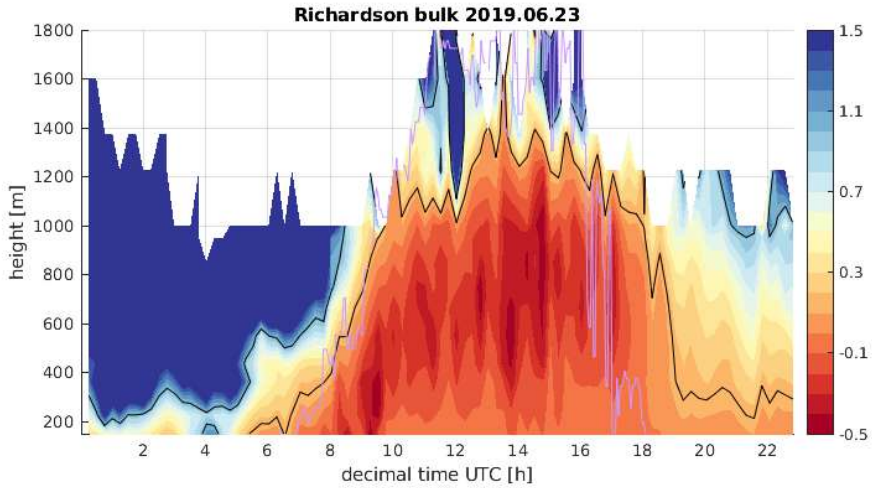

- Diurnal evolution of Ri_B with stable at nighttime conditions.
- Convection generally reaches slightly higher altitues than unstable values of Ri_B.
- Evolution of Ri_B shows diurnal cycle in which unstable conditions last later than daytime convective turbulence.

Universität zu Köln

Study cases: Ri_B in summer 2022 with heat wave

18.06.2022

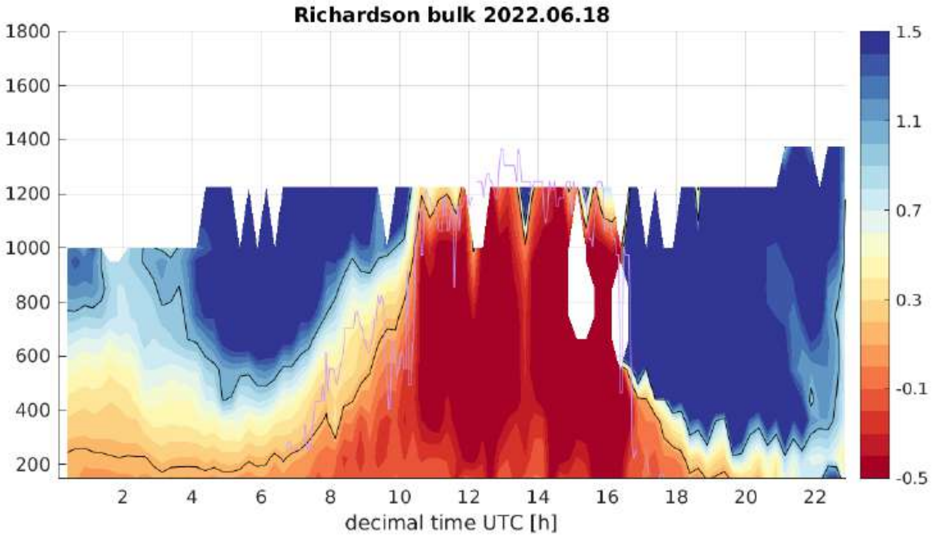

19.06.2022

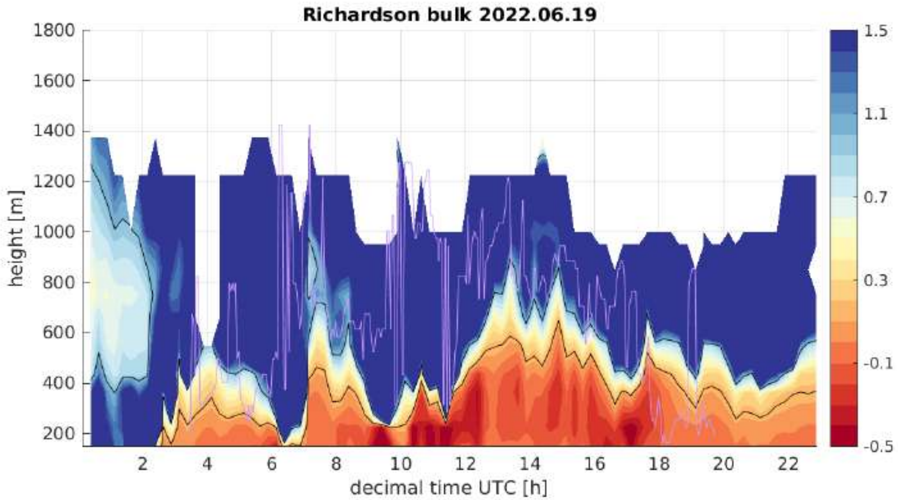

- Diurnal evolution of Ri_B show instability even at nighttime.

Study cases: summer 2022 with heat wave

17.06.2022

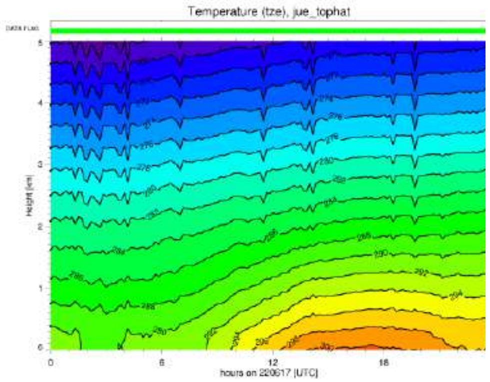

18.06.2022

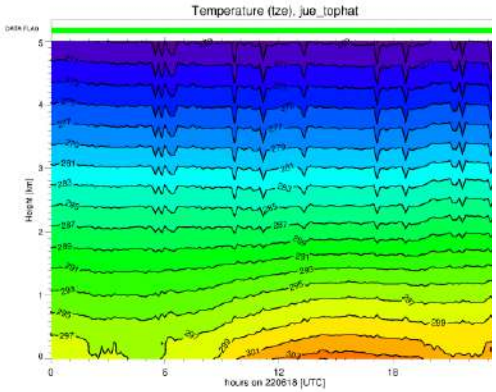

19.06.2022

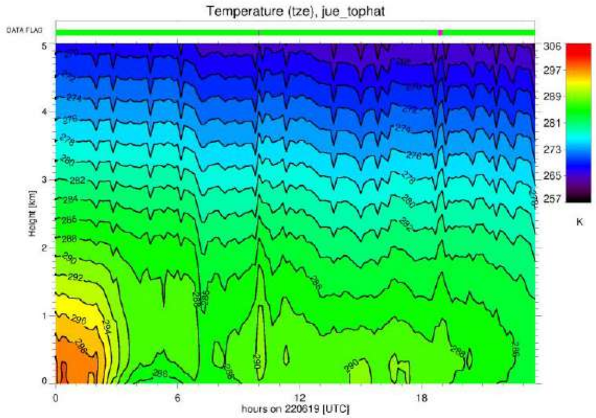

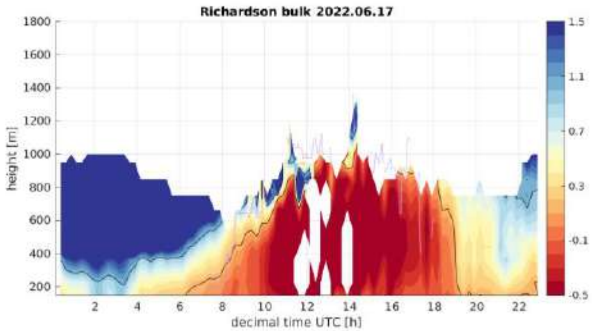

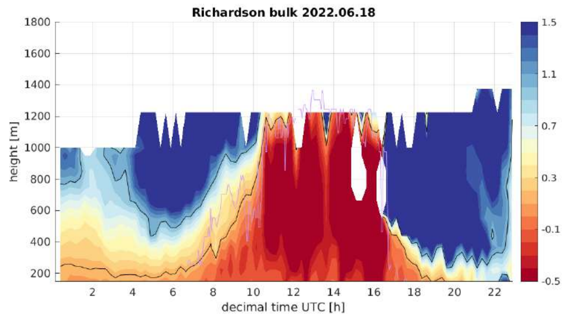

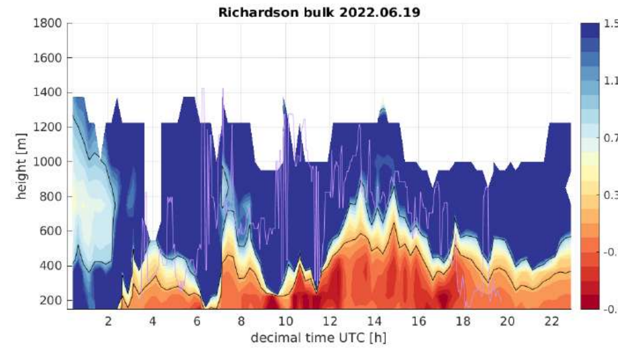

Universität zu Köln

Study cases: summer 2022 with heat wave

June 19 2022: end of heat wave

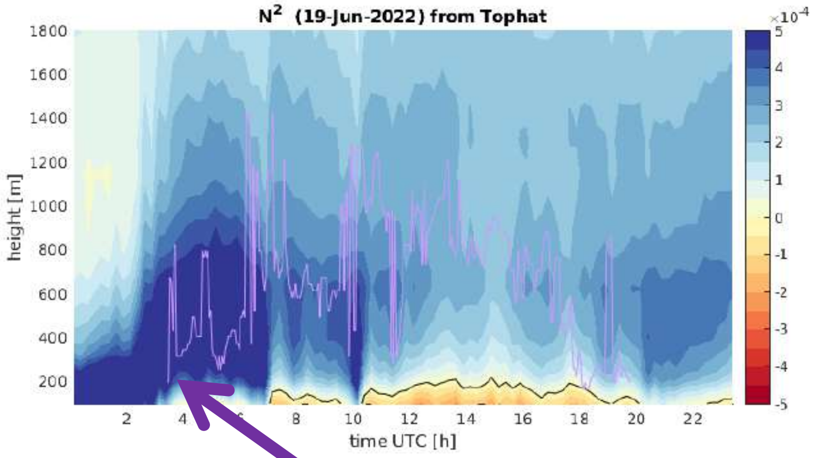

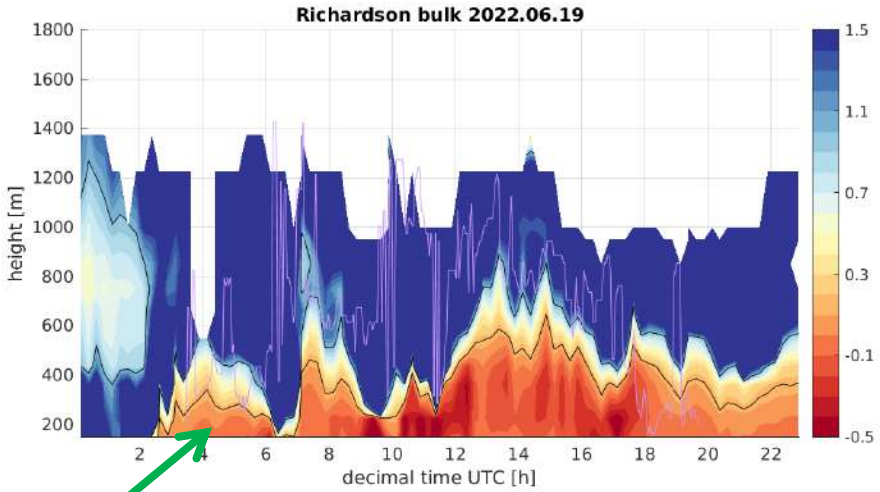

thermally very stable

low Ri_B values

- Thermally very stable at night but shear and convection are present.
- Unstable nighttime conditions visible in Ri_B.

Universität zu Köln

Sharp nighttime changes in June 19 2022

June 19 2022: end of heat wave

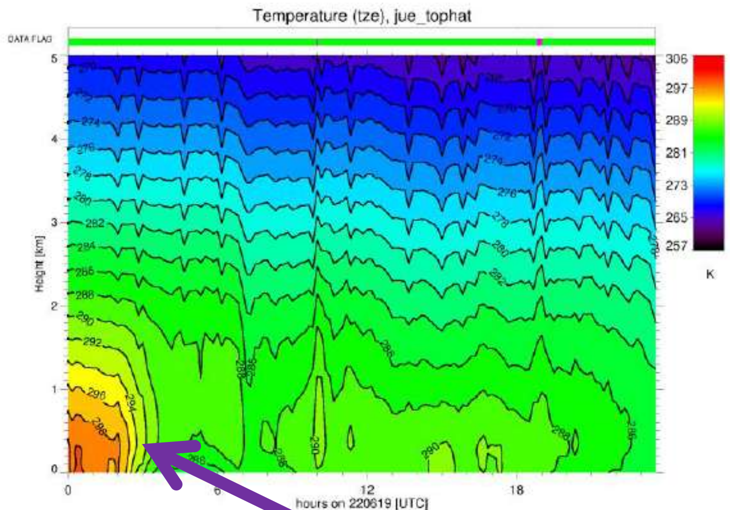

sudden end of heat wave

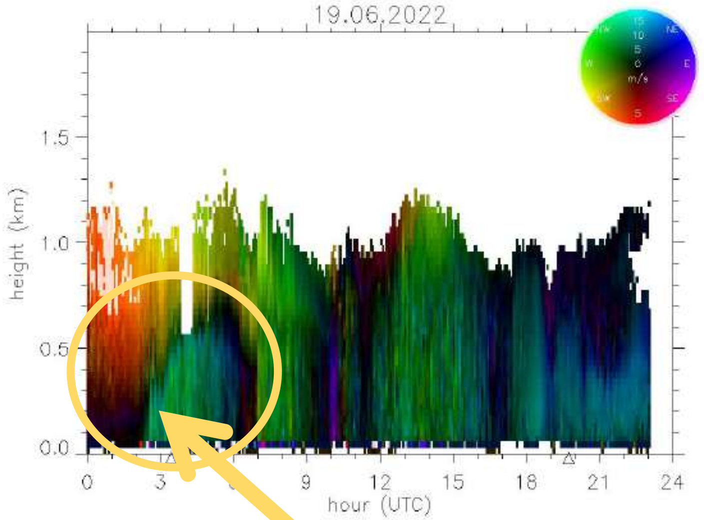

sharp change of wind direction

What other processes can we identify in ABL that can contribute to cool it and end the heat wave?

Work in progress: derive advection from MWR 30° scans

$$horizontal\ thermal\ advection = u\frac{dT}{dx} + v\frac{dT}{dy}$$

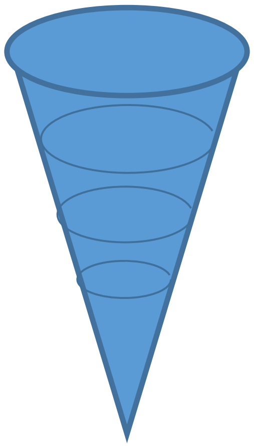

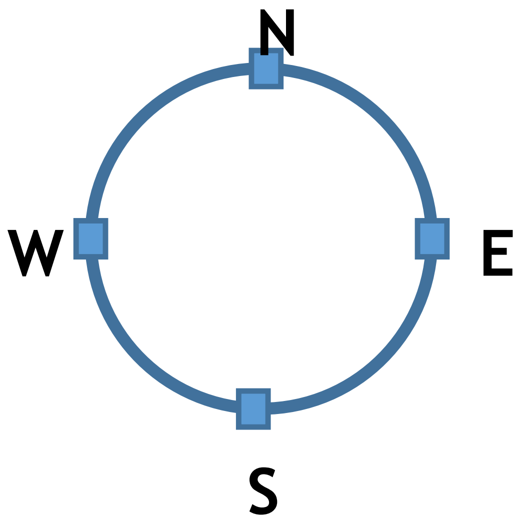

- At each height, a zonal and a meridional gradient of temperature is estimated.
- The evolution of advection is estimated within the ABL.

$$\frac{dT}{dx} = \frac{T_{East} - T_{West}}{x_{East} - x_{West}}$$

$$\frac{dT}{dy} = \frac{T_{North} - T_{South}}{y_{North} - y_{South}}$$

Horizontal thermal advection at end of heat wave

- Colder air advected from the North-West rapidly cools the ABL.
- Quantifying advection is important in order to identify the mixing mechanisms in the ABL.

zonal component

$$u\frac{dT}{dx}$$

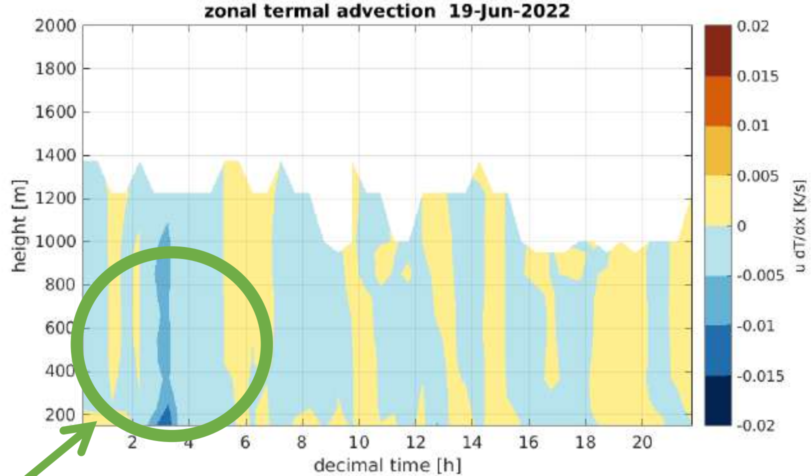

End of heat wave

meridional component

$$v\frac{dT}{dy}$$

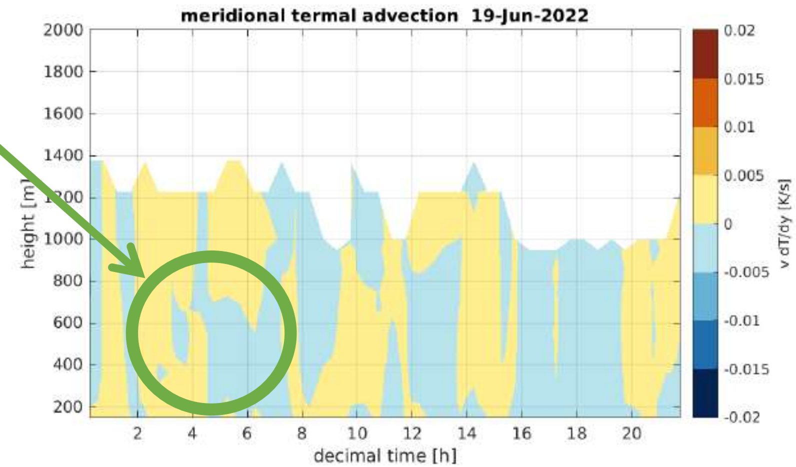

Conclusions and outlook

- A synergistic approach utilizing MWR and WDL in CCRES units is able to better elucidate the processes that determine the extent and structure of the ABL.
- This characterization of the ABL highly impact the transport of tracers and the formation of clouds.

Future:

- Investigation of sensible and latent surface heat fluxes in ABL employing highly resolved temperature and water vapor measurements (from Raman lidar) and velocities (from Doppler lidar).

Universität zu Köln

Thanks for your attention!

Questions? :)

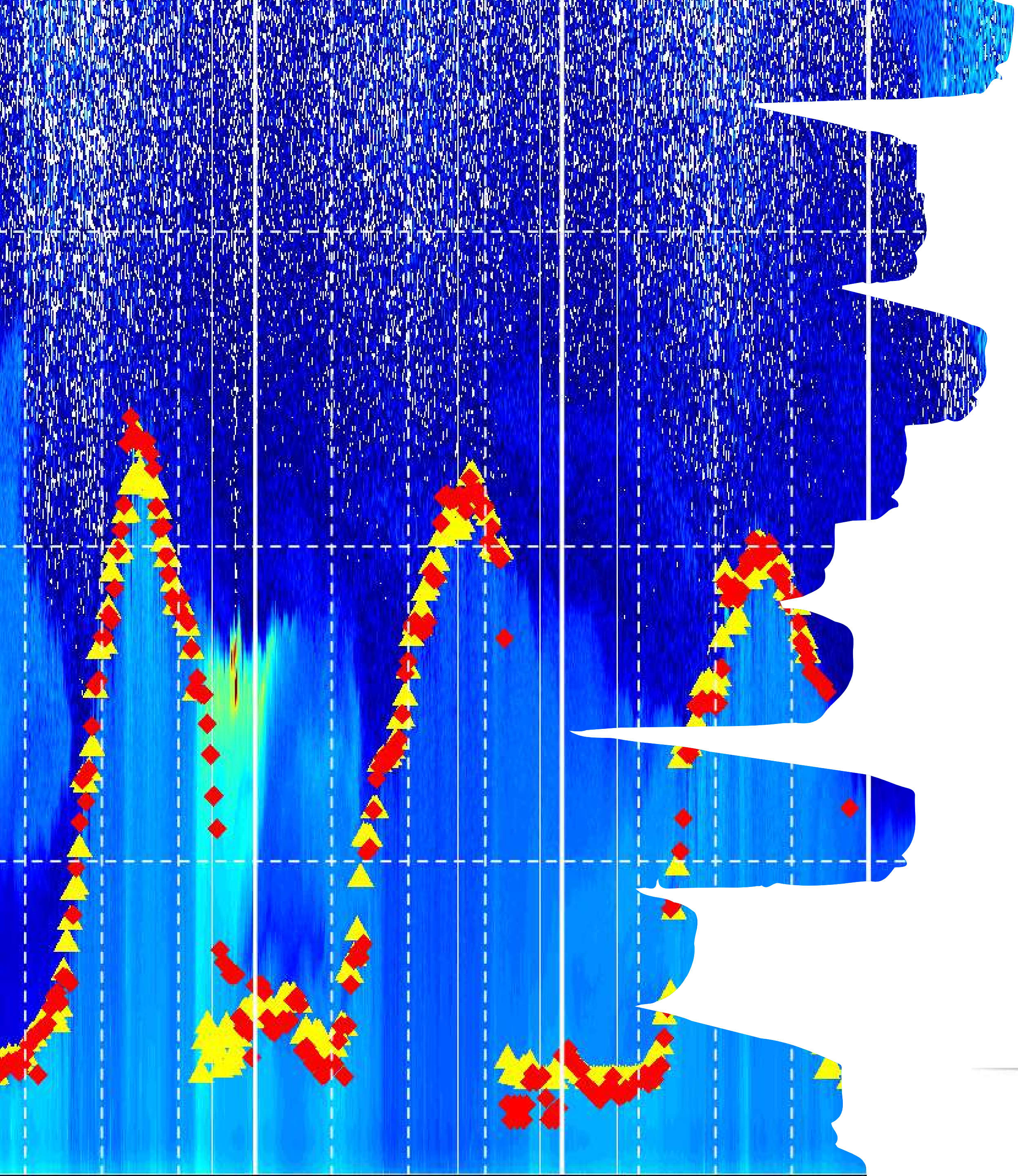

ACTRIS CCRES

ABL height detection

Simone Kotthaus & Melania Van Hove (IPSL)

CCRES Workshop, SIRTA – Nov 14-15th, 2022

This project receives funding from the European Union's Horizon 2020 research and innovation programme under grant agreements No 871115

ABL heights – potential applications

- Interaction of ABL dynamics with cloud processes
- Transport of pollutants (vertical dilution) and greenhouse gases
- Entrainment of elevated aerosol layers

Theeuwes et al. (2019)

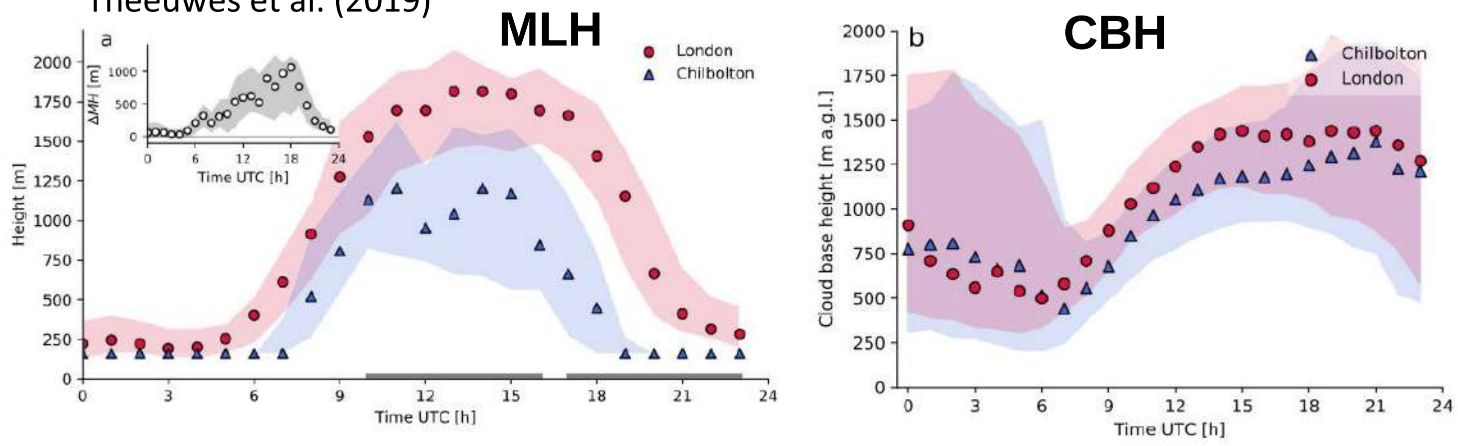

Foret et al. (2022)

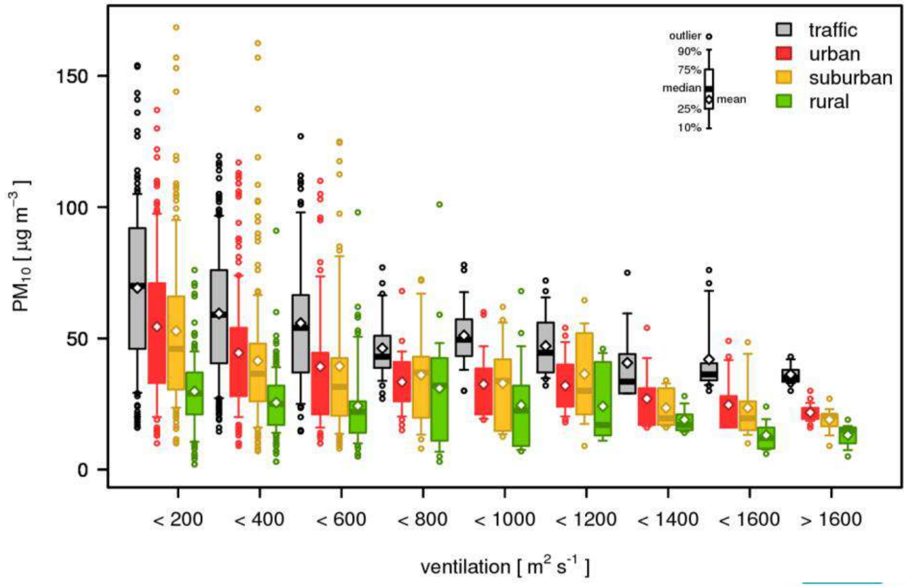

→ Urban area of London, UK: greater CBH associated with greater MLH
→ Enhanced vertical mixing over city leads to more persistent convective clouds during spring/summer afternoons compared to grass or croplands

→ Extreme winter-time surface-level PM_{10} in Paris only observed when ventilation coefficient is low (MLH x wind speed)

ACTRIS CCRES

How to diagnose ABL heights?

In-situ profiling

- Radiosondes: operational, global coverage, low temporal resolution
- UAS: emerging technology, not yet fully autonomous
- Towers: limited vertical extent
- Aircrafts: spatial displacement, limited temporal coverage

Ground-based remote sensing

- T (RH) profiling: MWR/IRS
- Humidity and trace gases: DIAL
- Wind & turbulence: DWL/SODAR/RADAR
- Aerosols: ALC

→ Capabilities and limitations summarised by [Kotthaus et al. (2022)]

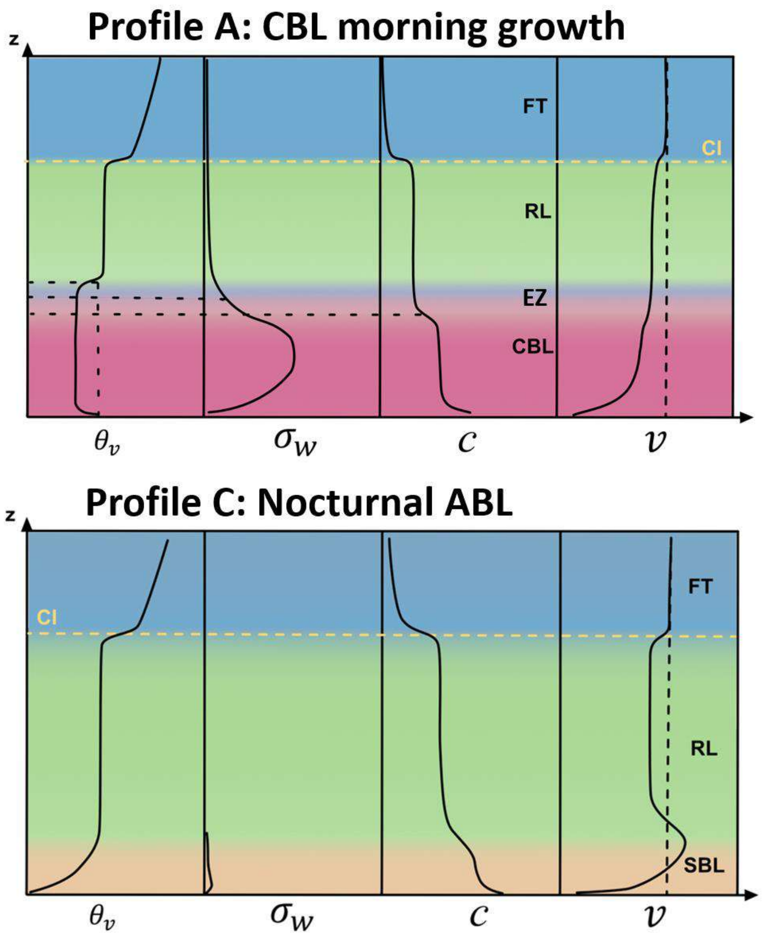

Kotthaus et al. (2022)

ACTRIS CCRES

Aerosol-based detection of ABLH and MLH

Tailored algorithms (Kotthaus et al. 2020):

STRATfinder for ALC with high SNR (e.g. CHM15k, CL61)

CABAM for ALC with low SNR (e.g. CL31)

STRATfinder

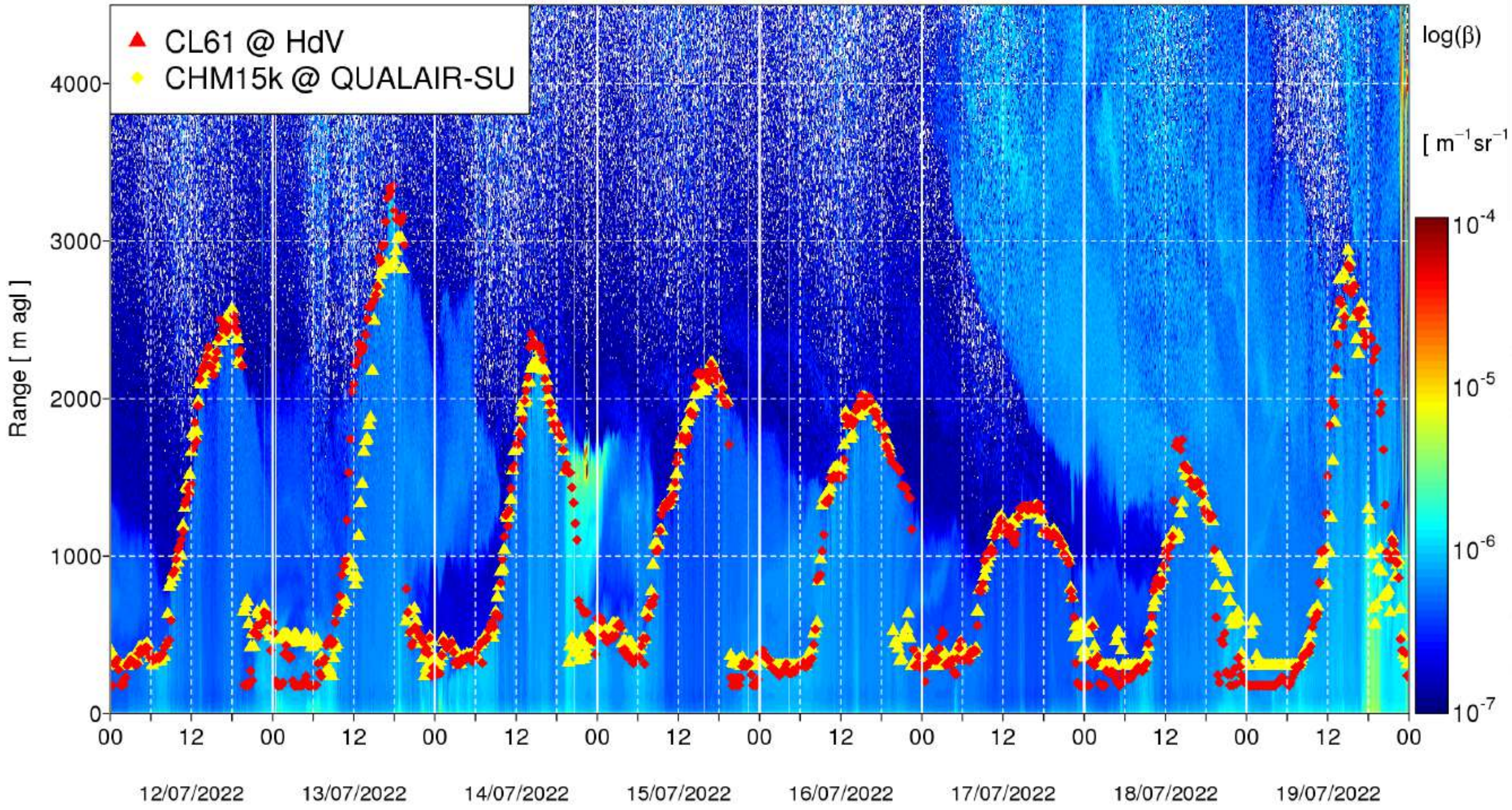

CABAM

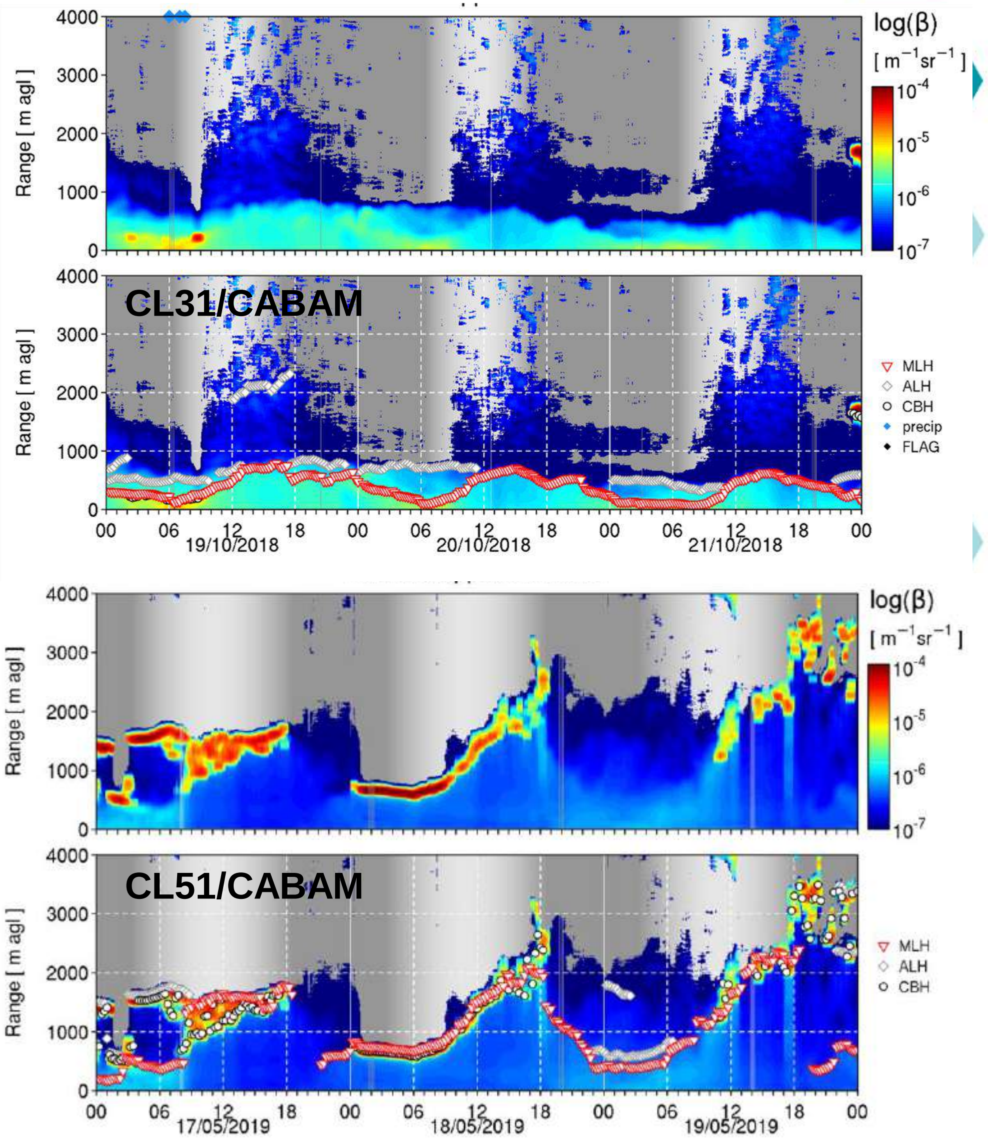

ABL testbed

Automatic retrieval of atmospheric boundary layer (ABL) heights from diverse sensor networks

Proof-of-concept

- Implementation at AERIS-ESPRI
- Diverse ALC, incl CL31, CL51, CL61, CHM15k
- Now testing CIMEL & miniMPL
- Supported by ACTRIS, ICOS, PROBE, …
- Careful pre-processing required

https://ablh.aeris-data.fr/

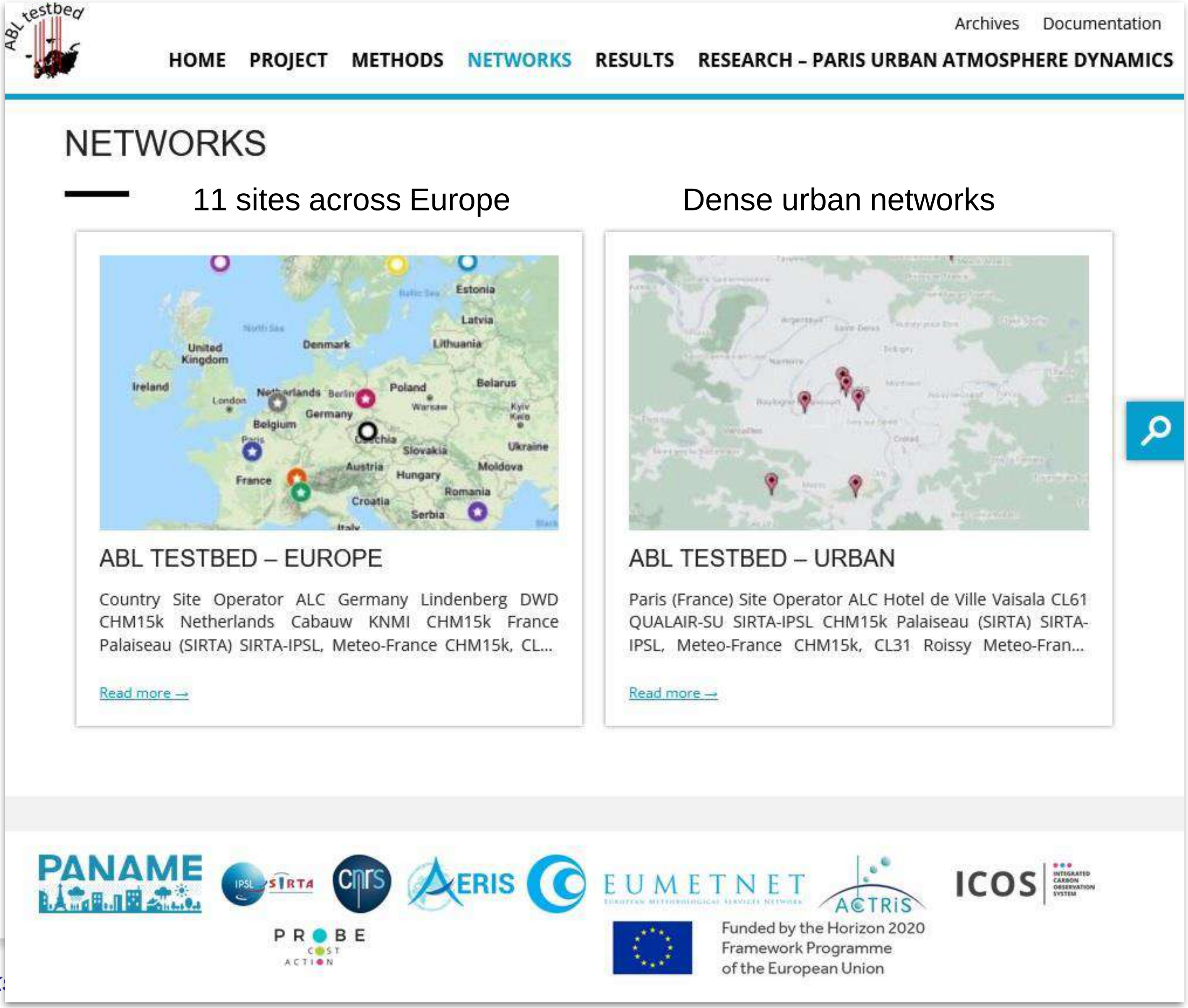

ACTRIS CCRES

ABL testbed – Europe: Processing status

ABL testbed – Europe
- 11 sites, 17 ALC
- Study period from early 2018
- L1 processing at E-PROFILE
- ALC corrections, calibrations, MLH detection at AERIS

CHM15k/STRATfinder | CL31/CABAM
CL61/STRATfinder | CL51/CABAM

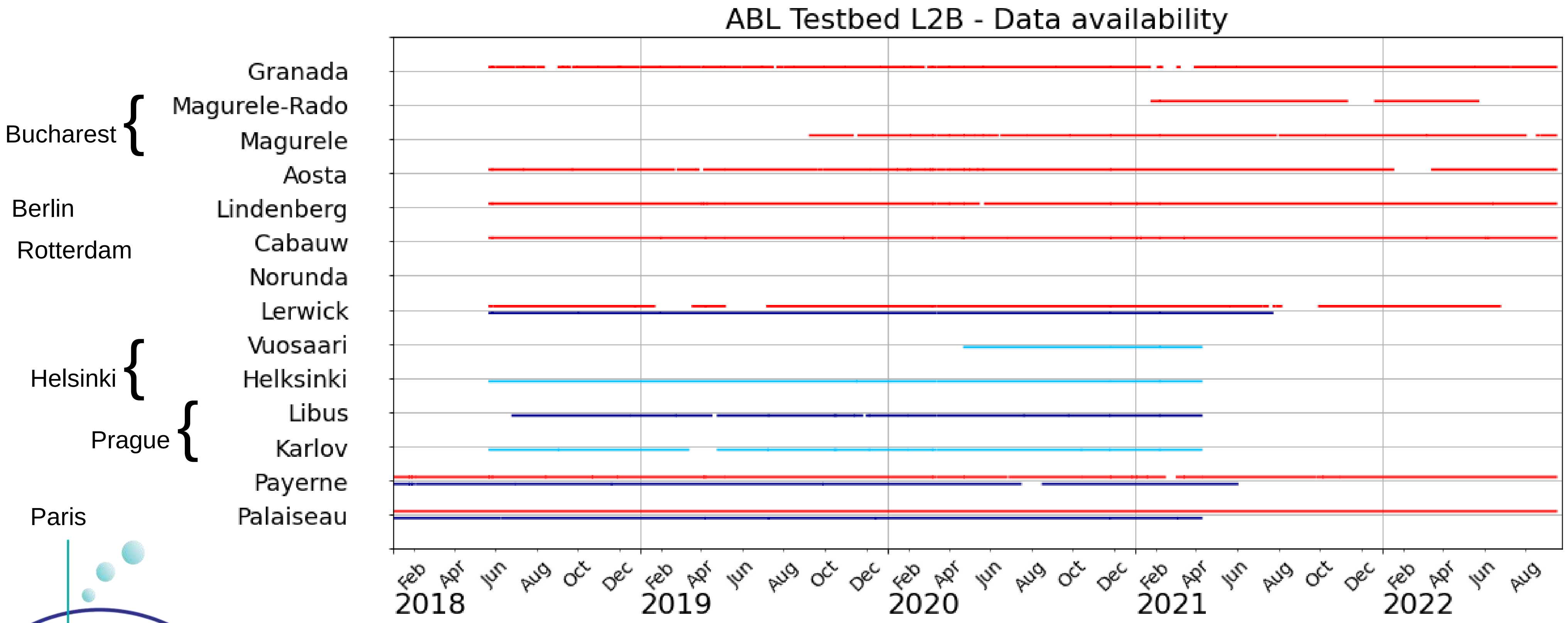

Diurnal and seasonal variations

Height of the total Atmospheric Boundary Layer and Mixed Layer @ IPSL SIRTA

2015-2021

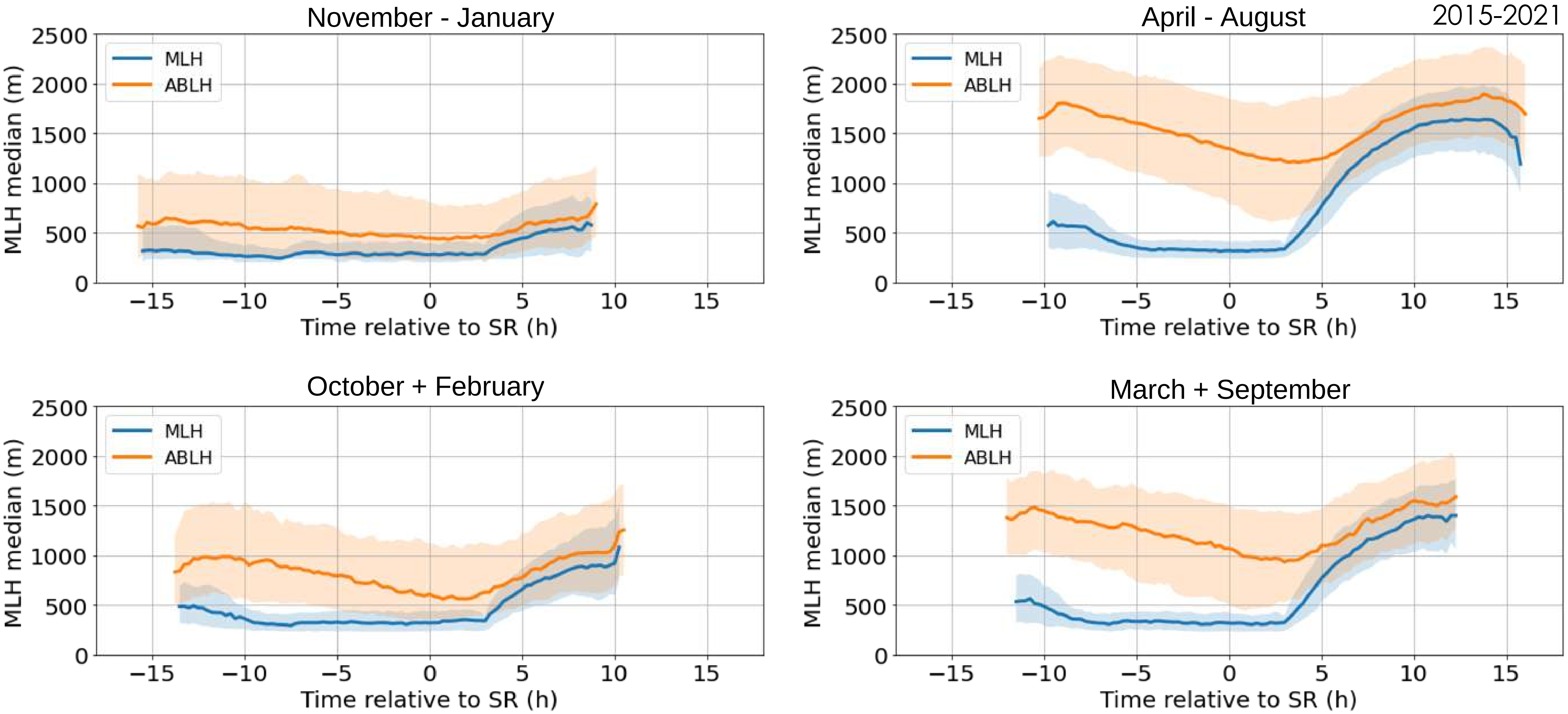

STRATfinder/CHM15k: v2022a

Algorithm / sensor performance

Methods inter-comparison

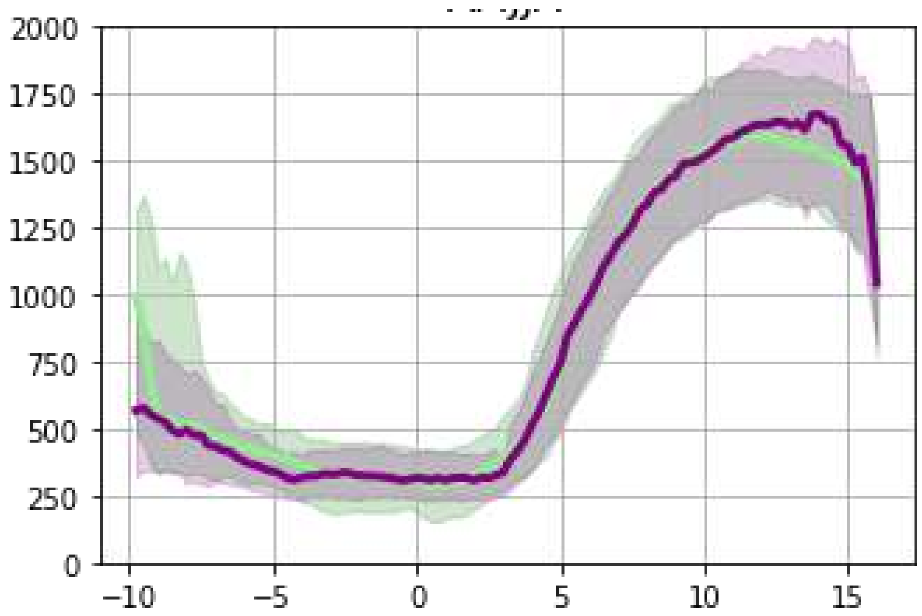

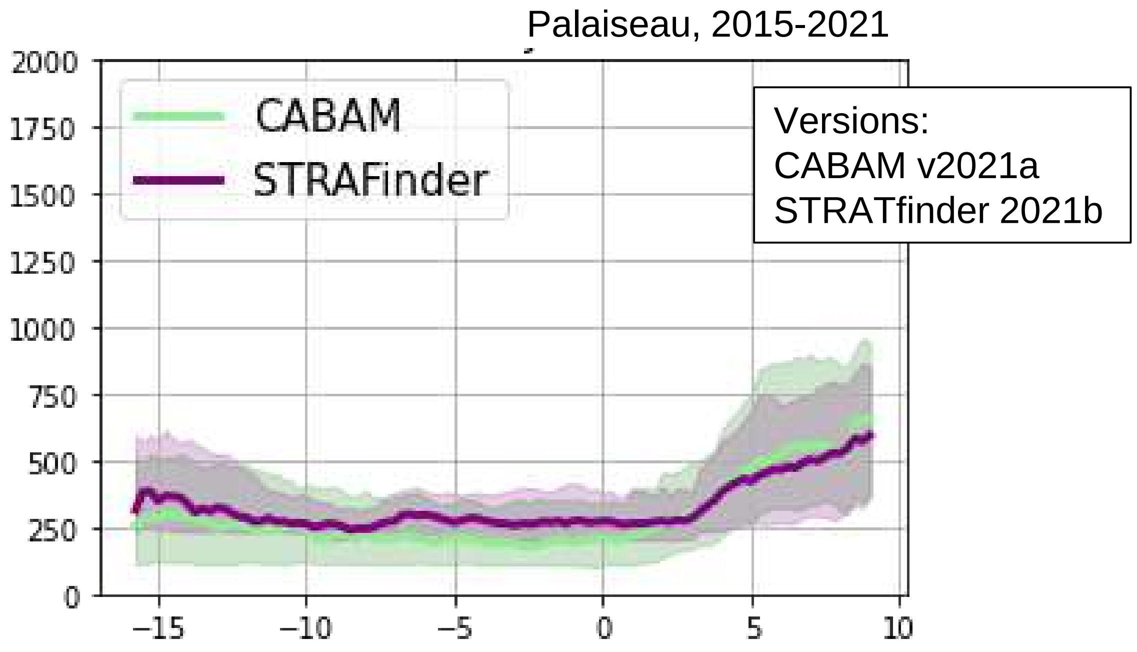

Performance - "take home messages"

- CABAM/CL31 reduced performance for detection of deep layers (> 2000 m)
- STRATfinder/CHM15k not very suitable for detection of shallow layers (< 300 m)

→ **both related to quality of the input data**

Algorithm / sensor performance

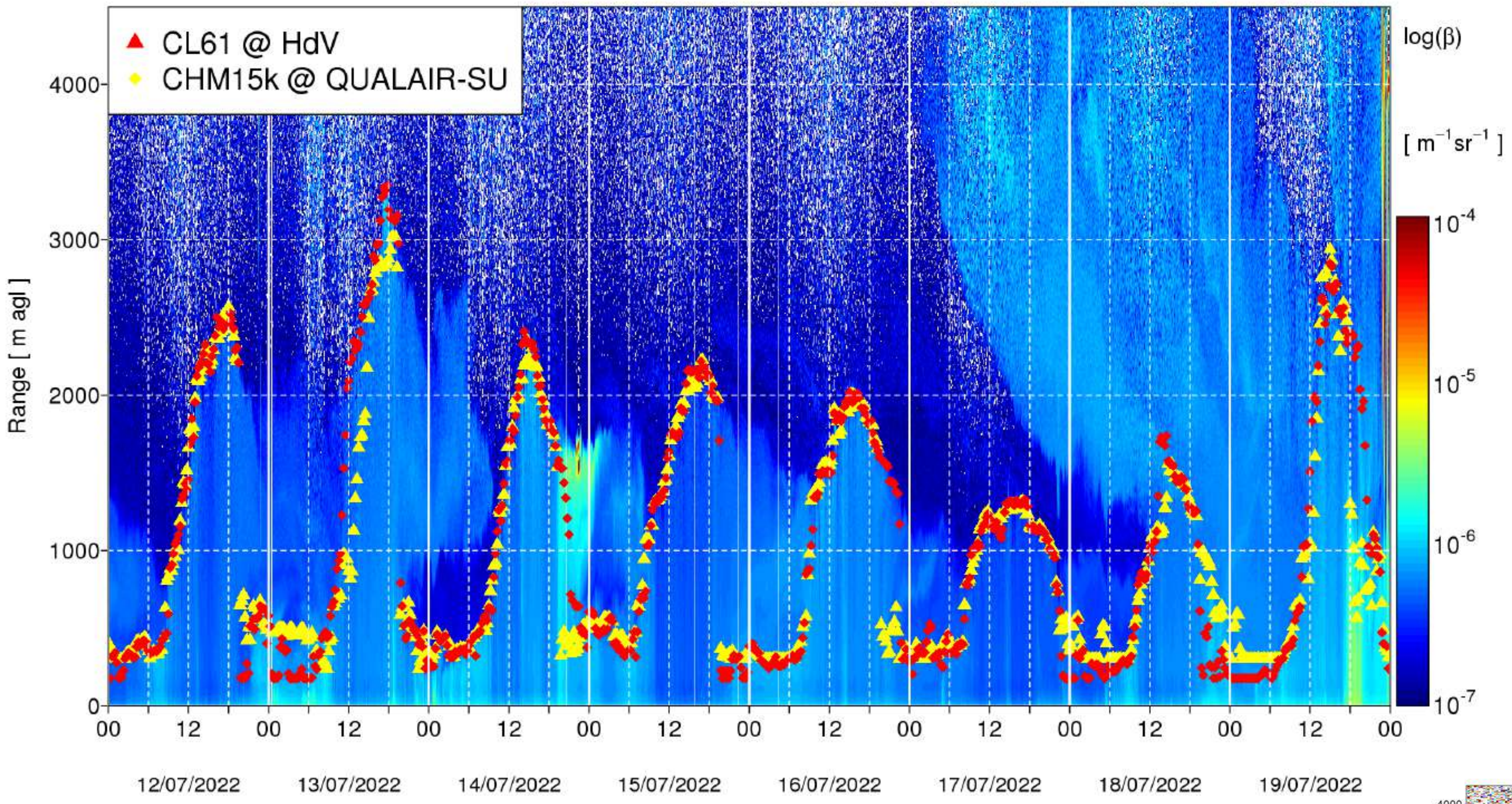

STRATfinder with CL61 or CHM15k

First results

- CL61 and CHM15k comparable SNR performance
- Improved detection of shallow layers with CL61
- Depol offers addition info (to be exploited in future)

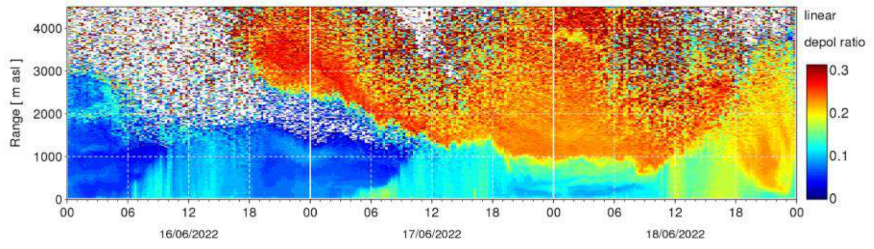

ACTRIS CCRES

Turbulence-derived heights

Observations:
J Cespedes
- Vaisala 400s
- QUALAIR-SU observatory in central Paris

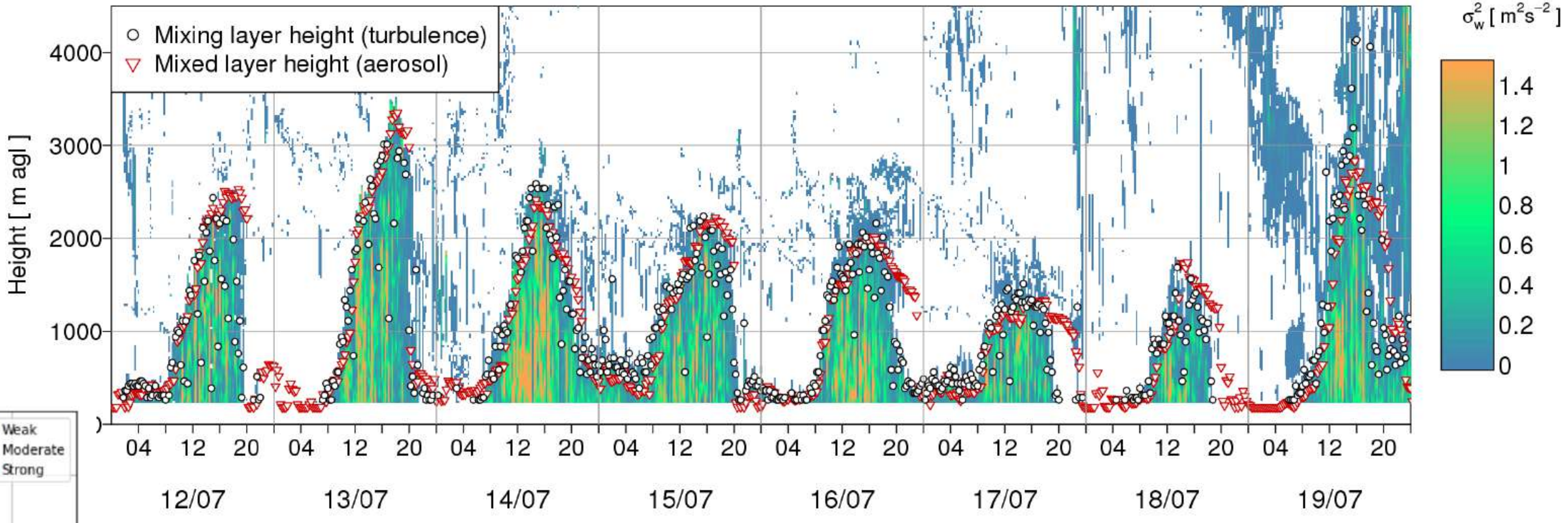

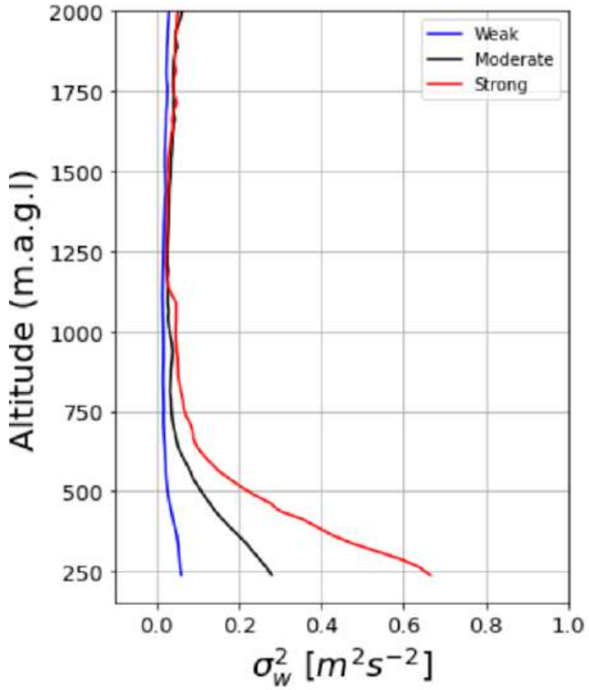

- Vertical velocity variance: direct measure of vertical mixing
- MH: profile value below certain threshold
- Implications of sampling frequency and calculation window?
- Implications of CNR thresholds (also for cloud/rainfall)
- QC: Temporal consistency

Next: thermodynamic retrievals incl MWR

Synergy for detection of ABL heights…

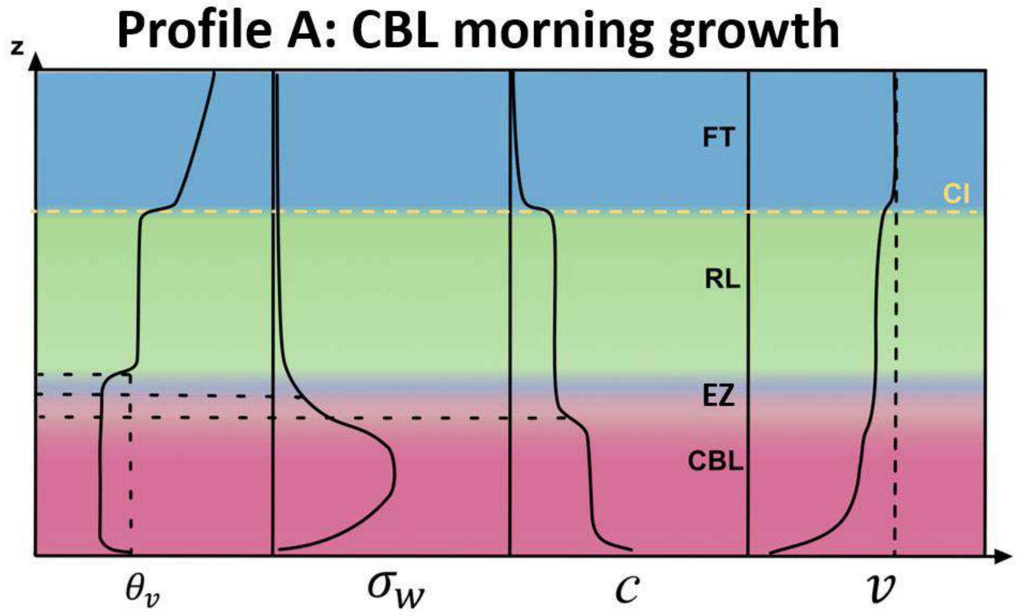

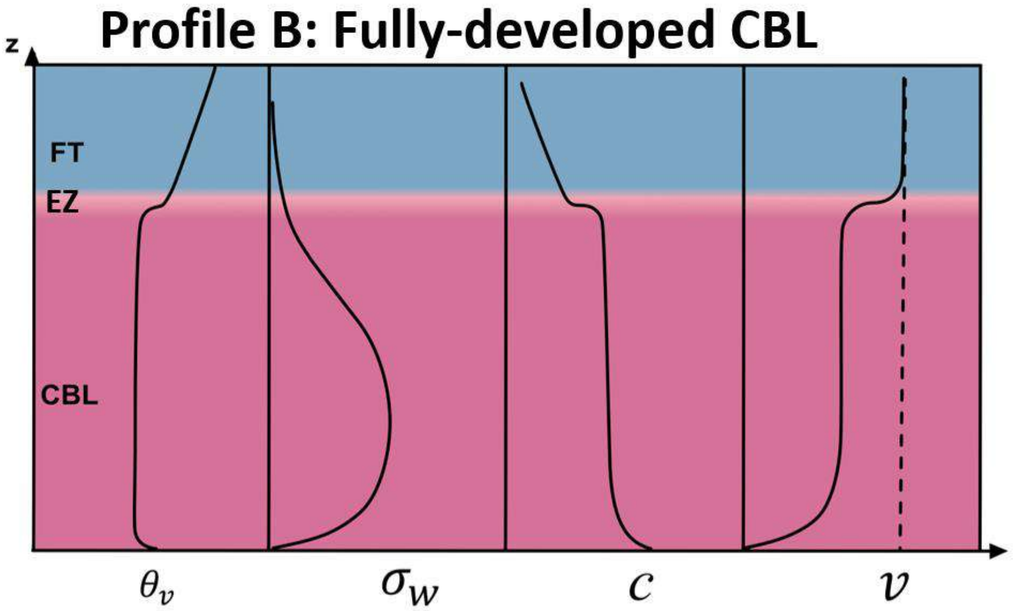

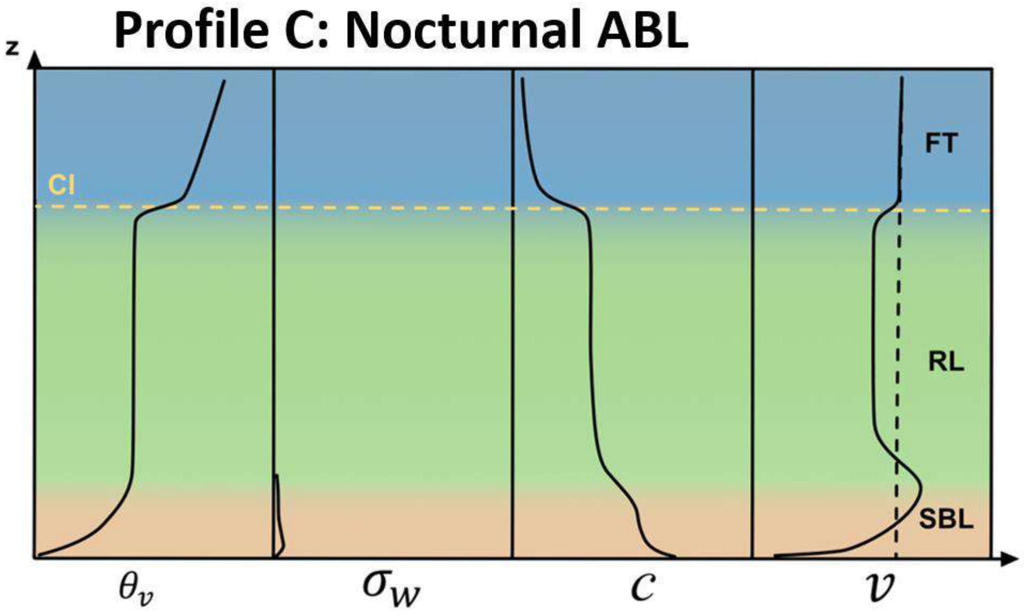

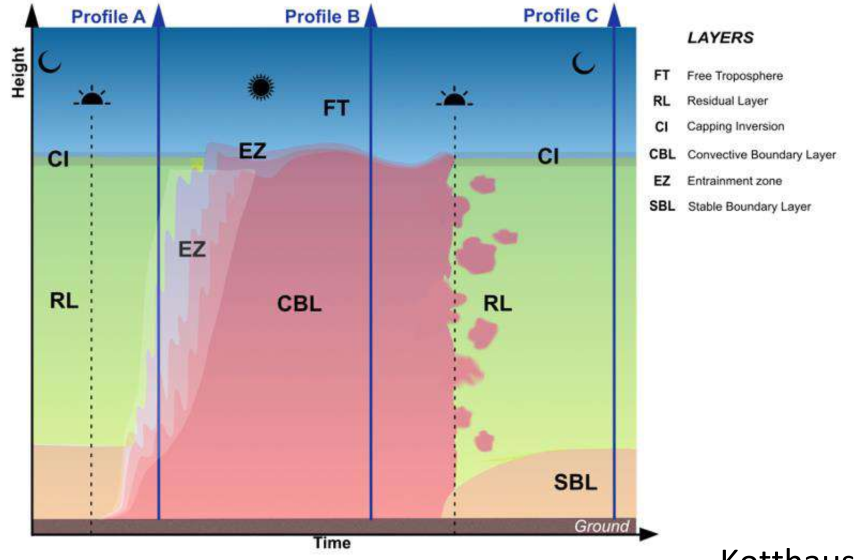

Kotthaus et al. (2022)

ACTRIS
CCRES

Thank you

Calibration transfer methodology for different band cloud radars

S. Jorquera, F. Toledo, J. Delanoë, A. Berne, A-C. Billault-Roux, A. Schwarzenboeck, F. Dezitter, N. Viltard and A. Martini

Motivation

- Absolute calibration methods are time and labor intensive
- Calibration transfer is simple to set up
- Lack of standardized, repeatable methodologies for calibration transfer between different band radars

Calibration transfer principle

- Two radars sample clouds side by side
- A Correction Coefficient (CC) is identified to correct the reflectivity measurements of one radar, using the other as a reference

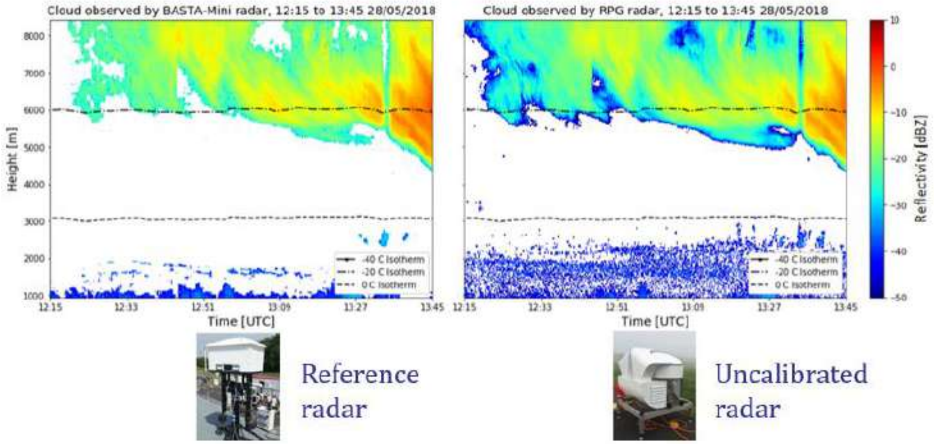

$$Z_r(r) = Z_u(r) + CC$$

Reference radar reflectivity

Uncalibrated radar reflectivity

Radar correction coefficient

Important considerations

- A simple linear regression is not enough to retrieve the CC
- Several factors may introduce noise or biases :
  - Differences in the sampling volume, low data correlation
  - Differences in the scattering regime between different band radars
  - Differences in atmospheric and hydrometeor attenuation at different frequency bands
  - Different radar sensitivities

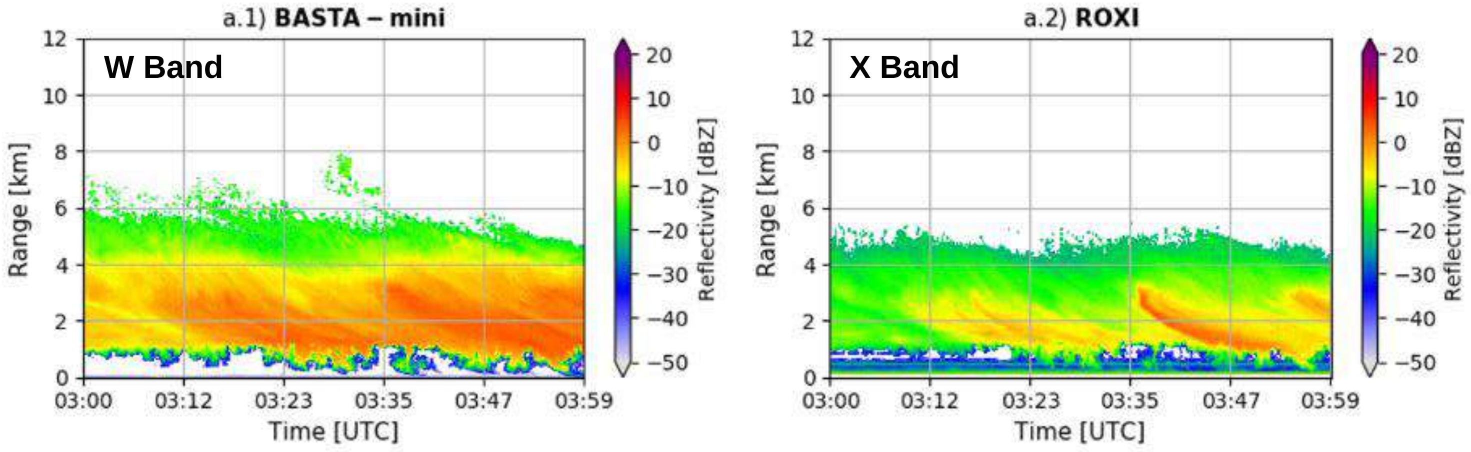

Important considerations

- A simple linear regression is not enough to retrieve the CC
- Several factors may introduce noise or biases :
  - Differences in the sampling volume, low data correlation
  - Differences in the scattering regime between different band radars
  - Differences in atmospheric and hydrometeor attenuation at different frequency bands
  - Different radar sensitivities

Ka band reflectivity

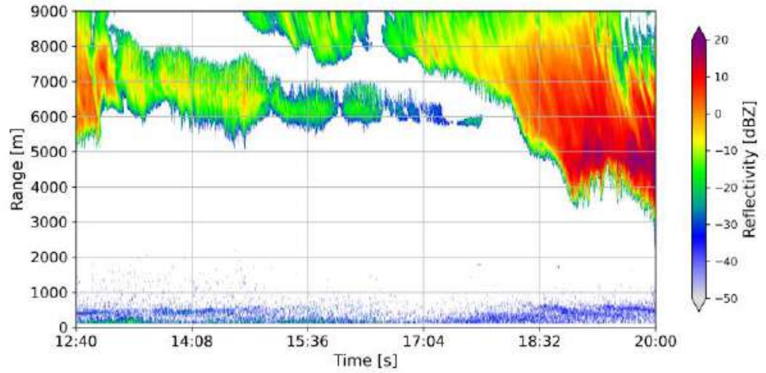

W band reflectivity

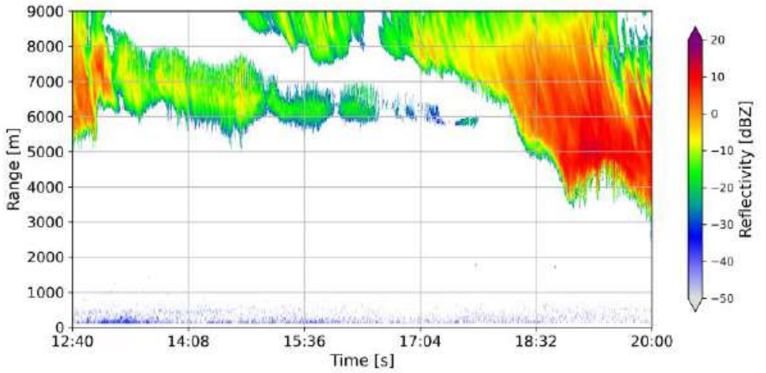

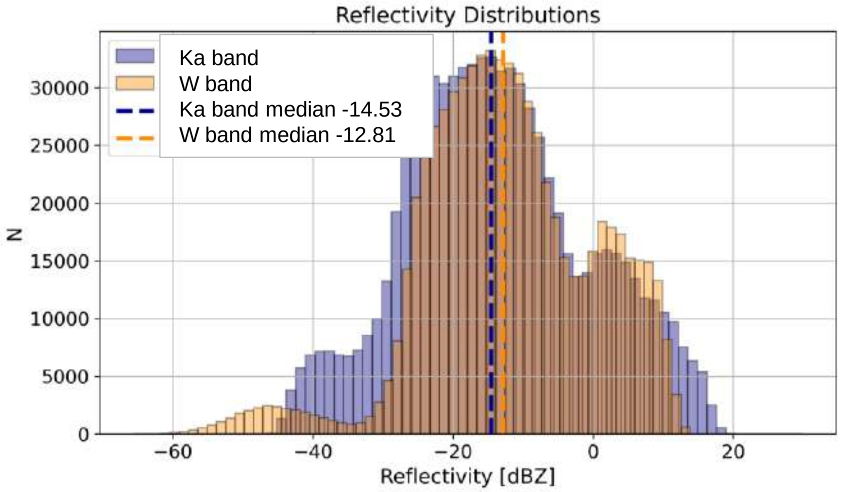

Methodology overview

- A methodology must be put in place to perform the calibration transfer without introducing biases in the resulting values

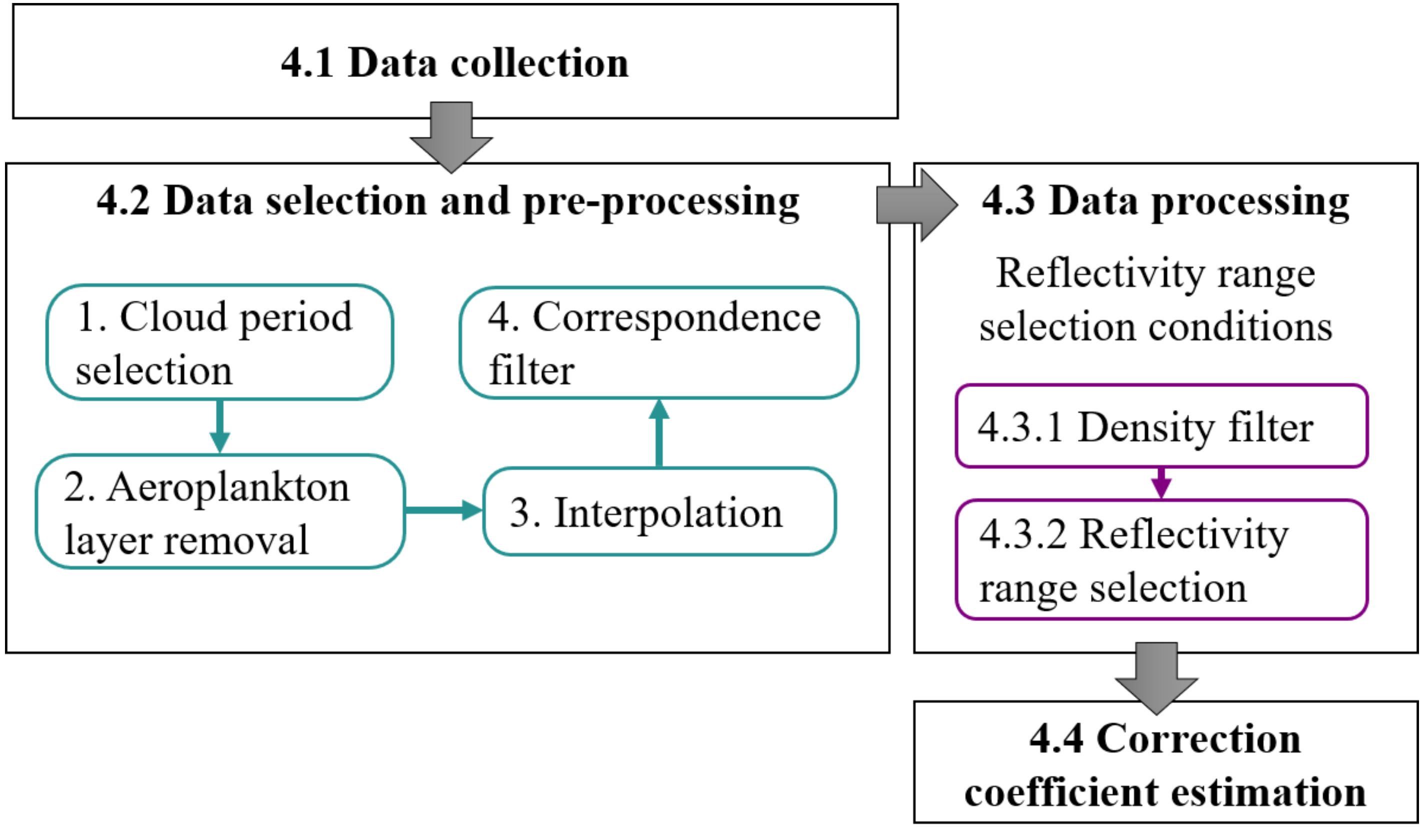

Data Collection

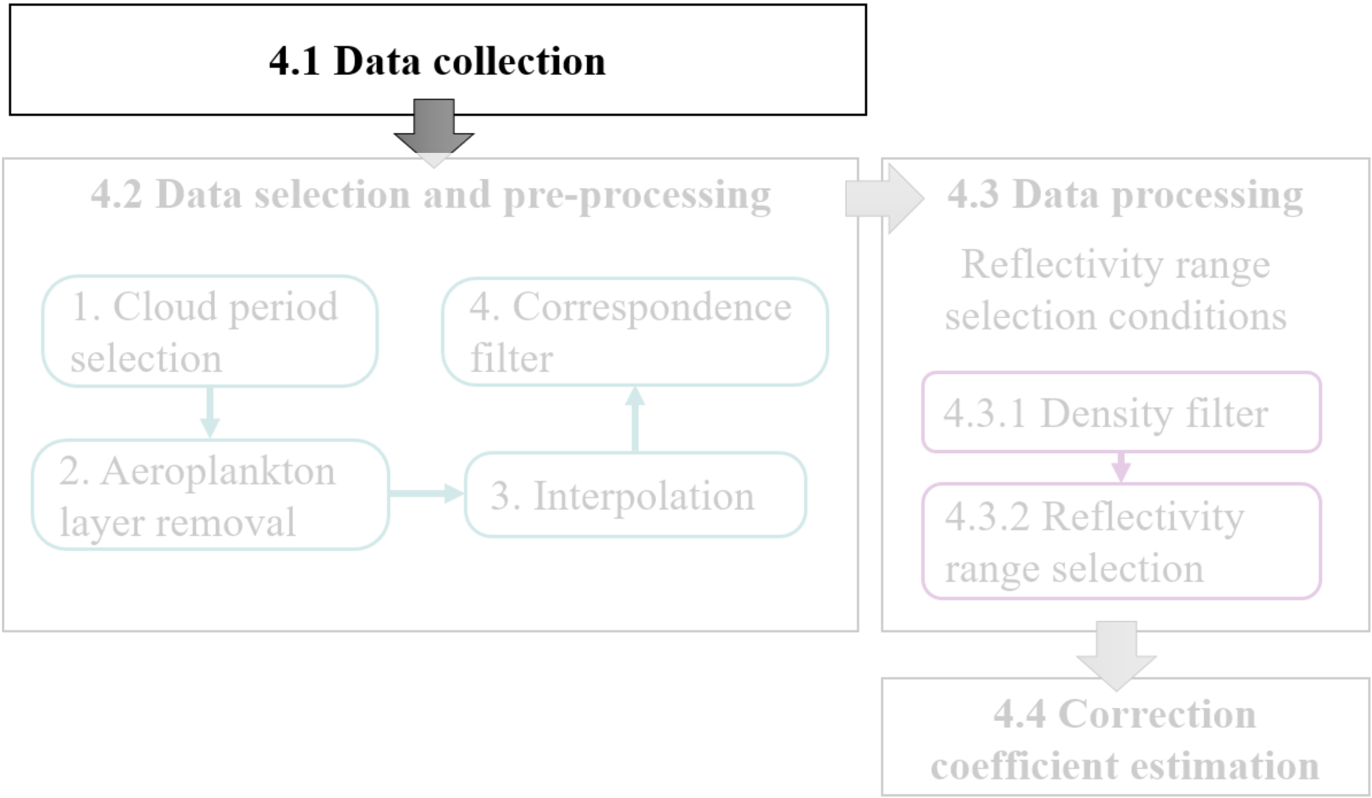

Data Collection

- Radars must be installed within a few tens of meters
- Radar interference must be avoided
- Simultaneous cloud sampling for a few days
  - 2 weeks is a good reference for sites that behave like SIRTA
- Attenuation due to atmospheric gases must be corrected
  - Gas profiles from weather models, radiosondes or microwave radiometers

Data Collection

- This methodology is developed based on results from the ICE-GENESIS campaign
- 4 radars were installed at Les Eplatures airport, in the Swiss Jura (1040 masl)

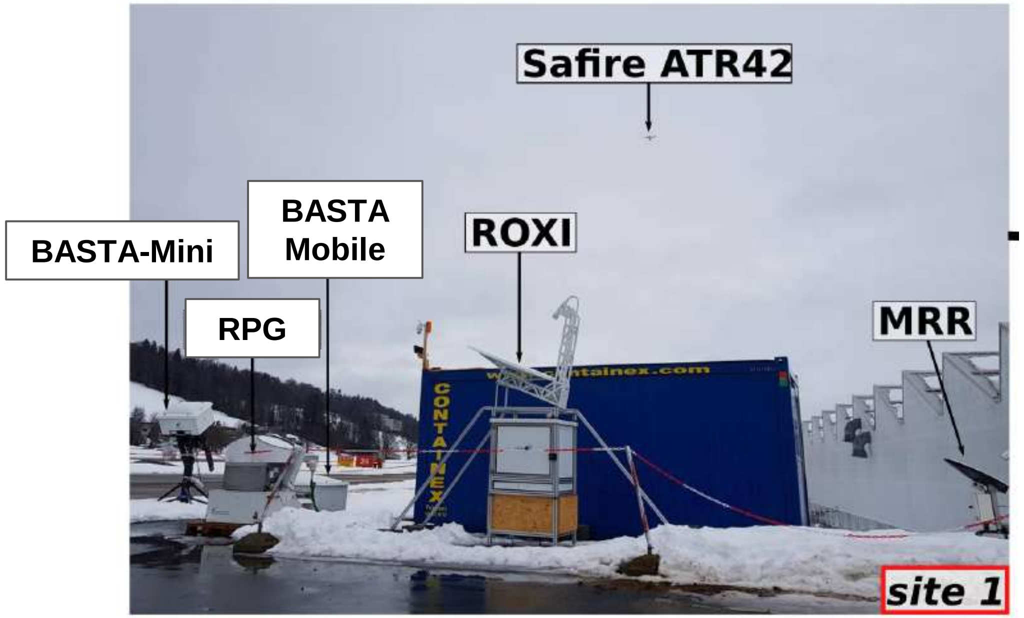

Billault-Roux, A.-C., and Coauthors, 2022: **Ice genesis: Synergetic aircraft, ground-based, remote sensing and in-situ measurements of snowfall microphysical properties** [manuscript submitted for publication]

Data Collection

- The method is developed based on results from the ICE-GENESIS campaign [1]
- 4 radars were installed at Les Eplatures airport, in the Swiss Jura (1040 masl)

Radar	Operating characteristics
BASTA-mini W band	Vertical range: 12000 m Range resolution: 12.5 m Frequency: 95.82 GHz Time resolution: 1 s Beam width: 0.8°
BASTA-mobile W band	Vertical range: 12000 m Range resolution: 12.5 m Frequency: 94.68 GHz Time resolution: 1 Beam width: 0.4°
RPG W band	Vertical range: 10000 m Range resolution: 7.5 / 16 / 32 m Frequency: 94.0 GHz Time resolution: 5 s Beam width: 0.48°
ROXI X band	Vertical range: 6400 m Range resolution: 50 m Frequency: 9.42 GHz Time resolution: 3 s Beam width: 1.86°

Data selection and pre-processing

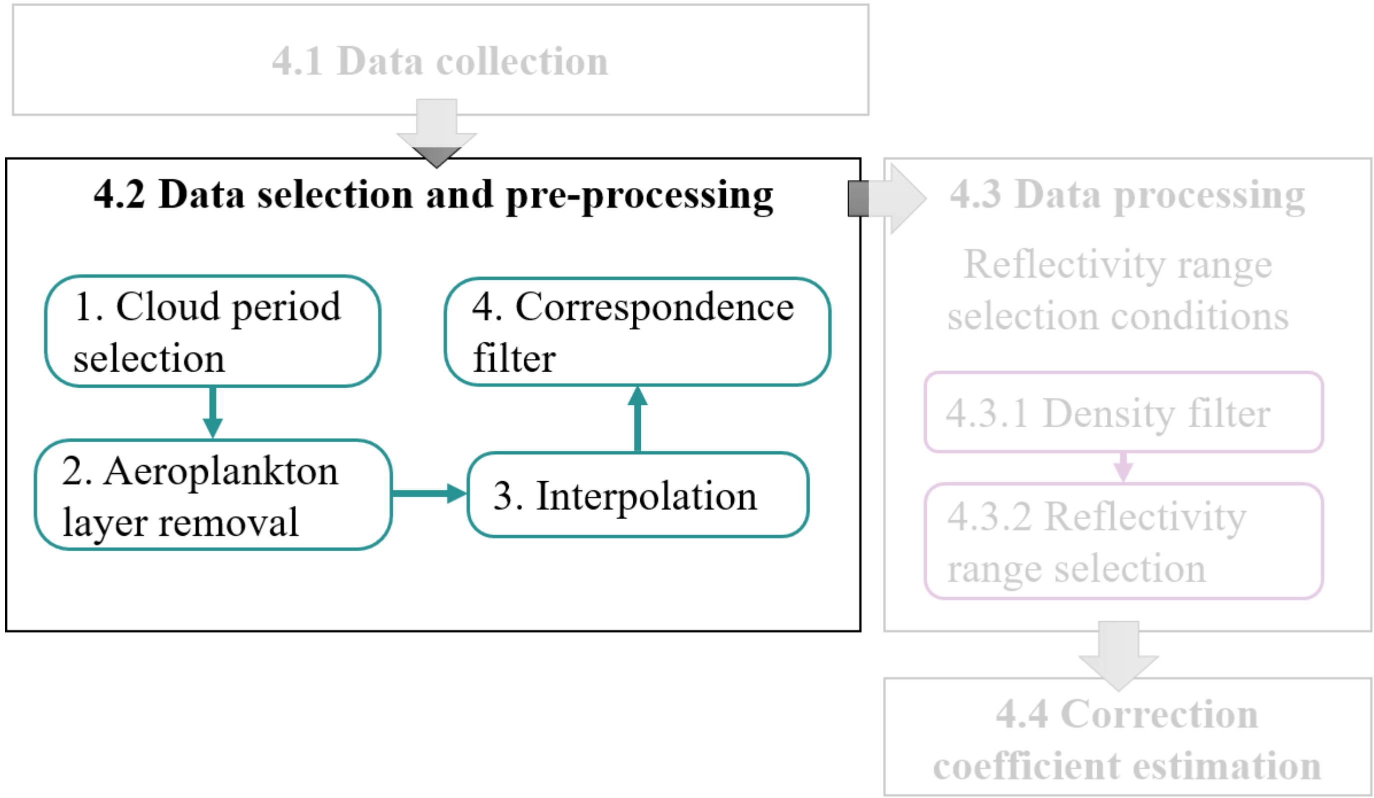

Data selection and pre-processing

- Clouds must be detected on both radars
- Ice clouds are preferred when transferring calibration between different frequency bands
  - To avoid differences in attenuation due to liquid hydrometeors
- Aeroplankton layer removal
  - Low correlation data
- Interpolation and correspondence filter
  - Comparison of corresponding samples only

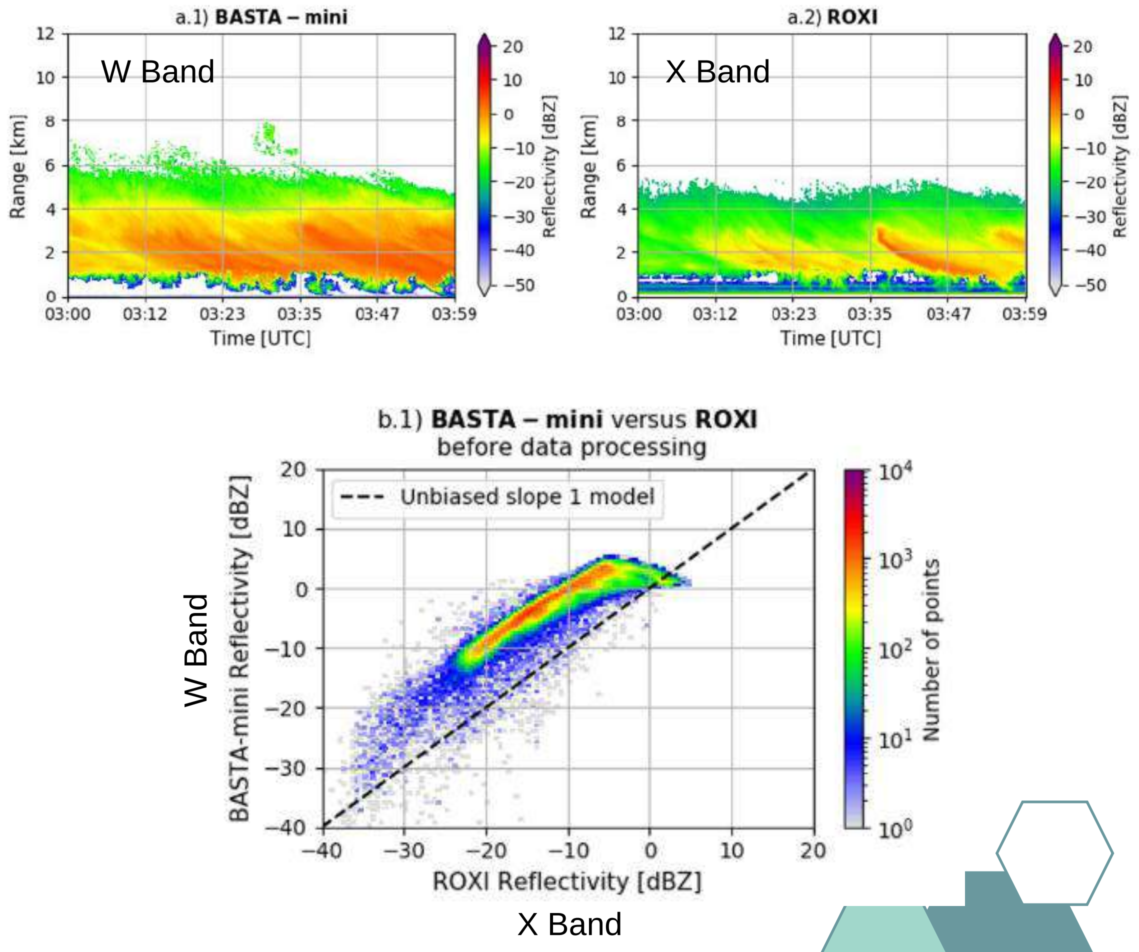

Data processing

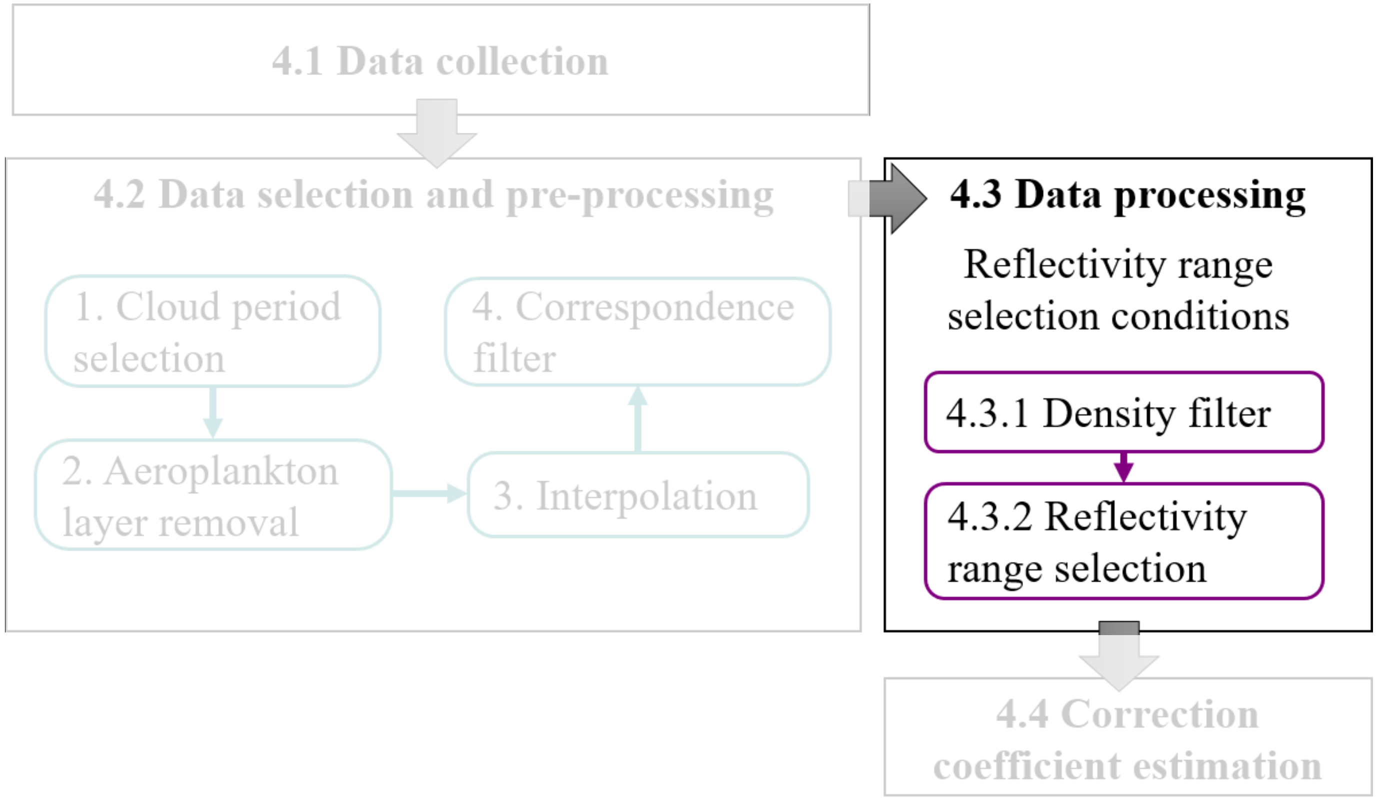

Data processing: Density filter

- Density filter
  - Removes data pairs with low repeteability (lower histogram density)

  - 2.5% of data pairs are removed

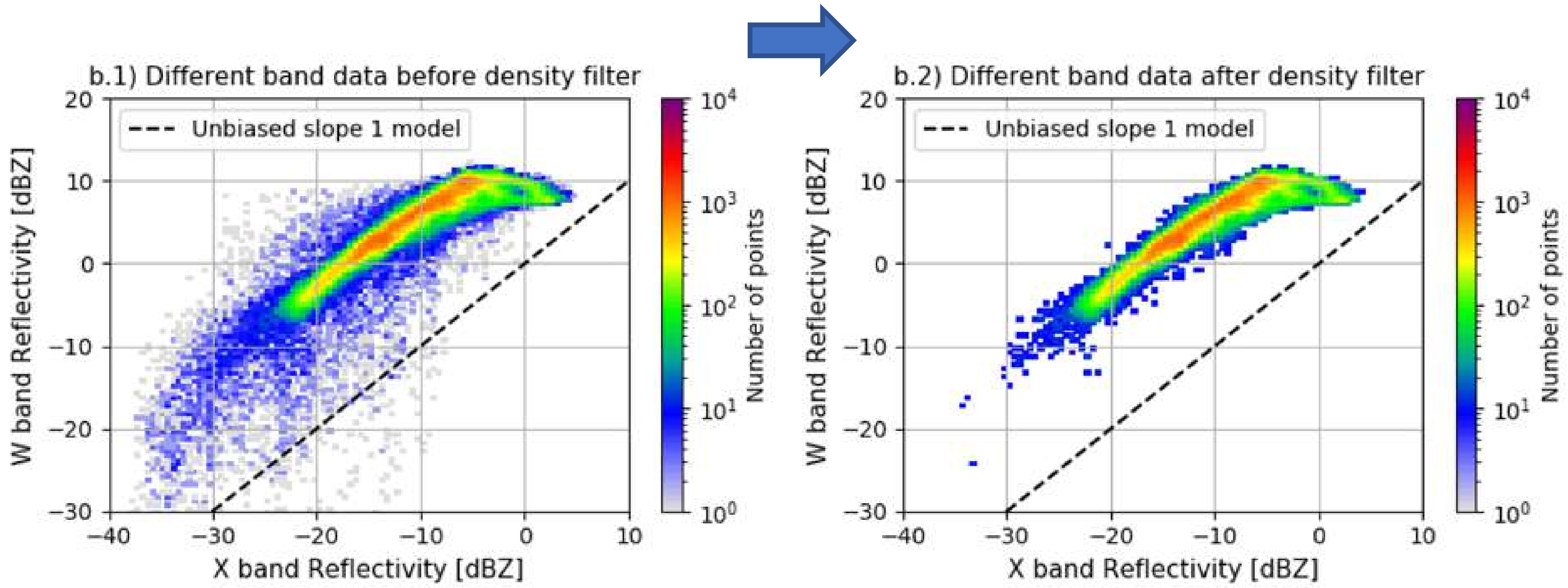

Data processing : Reflectivity range selection

- Reflectivity range selection
  - A correct comparison assumes a $y = 1 \cdot x + b$ model

$$Z_r(r) = Z_u(r) + CC$$

  - Can this be applied to different band radars?

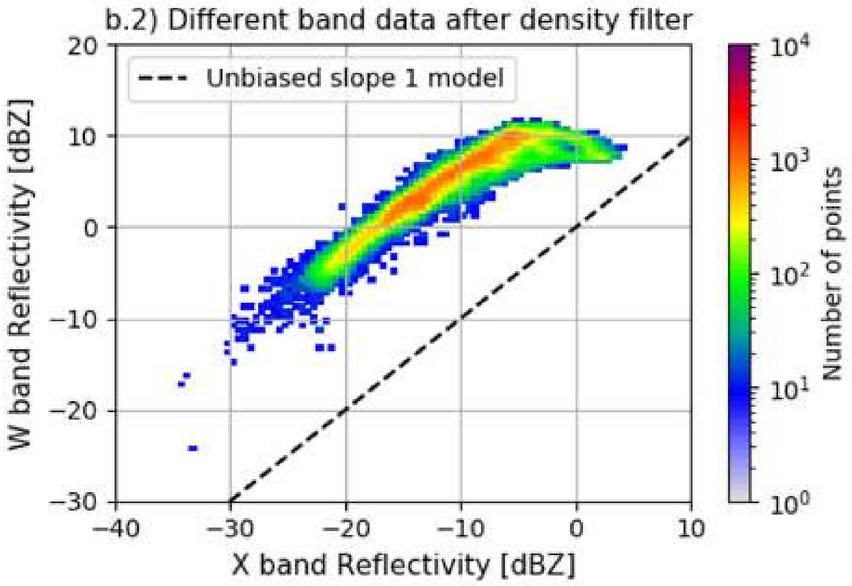

Data processing : Reflectivity range selection

- Reflectivity range selection
  - A correct comparison assumes a $y = 1 \cdot x + b$ model

$$Z_r(r) = Z_u(r) + CC$$

  - Does this apply to different band radars?
    - Yes, in some cases and for some reflectivity ranges
    - Empirically tested using in-situ ice particle data from clouds and the T-Matrix model
(HAIC measurement campaigns)

Haggerty, E. Defer, A. D. Laat, K. Bedka, J.-M. Moisselin, R. Potts, J. Delanoë, F. Parol, A. Grandin, and S. Divito. **Detecting clouds associated with jet engine ice crystal icing**. Bulletin of the American Meteorological Society, 100(1):31 – 40, 2019a. doi: 10.1175/BAMS-D-17-0252.1.URL https://journals.ametsoc.org/view/journals/bams/100/1/bams-d-17-0252.1.xml.

W and X band simulated reflectivity distribution for real ice particles

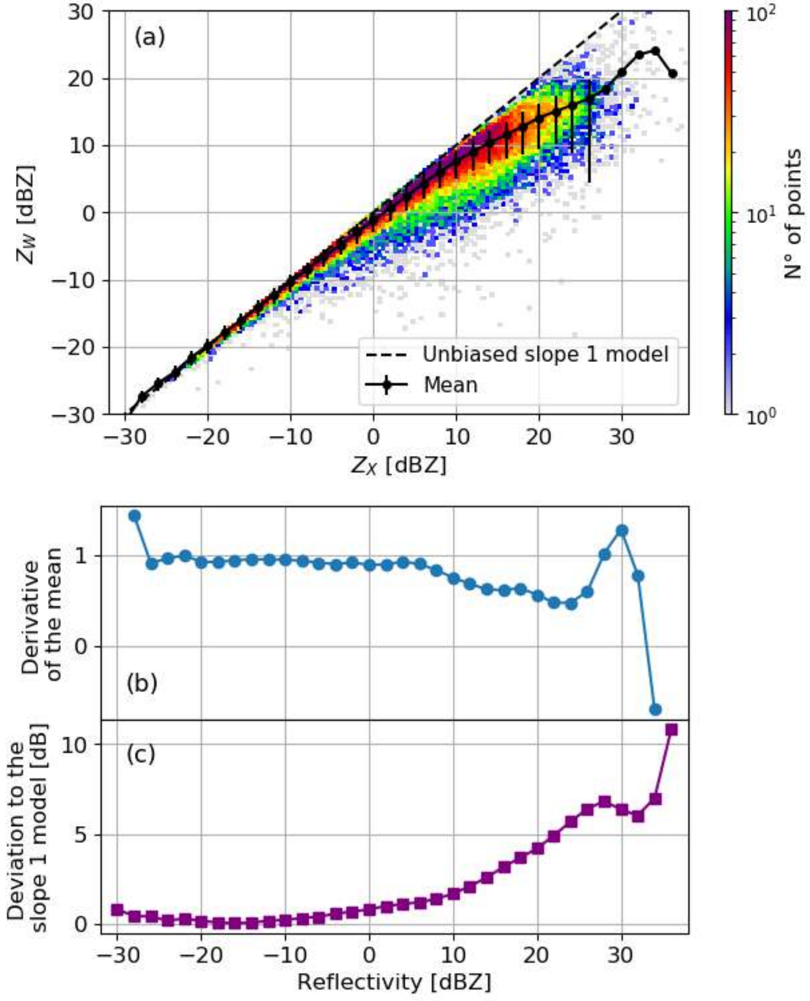

Data processing : Reflectivity range selection

- Reflectivity range selection
  - A correct comparison assumes a $y = 1 \cdot x + b$ model

$$Z_r(r) = Z_u(r) + CC$$

  - Afformentioned behavior is also observed when comparing W and X band radar samples

  - The departure from the slope 1 model must be accounted for before the calibration transfer

W and X band simulated reflectivity distribution for real ice particles

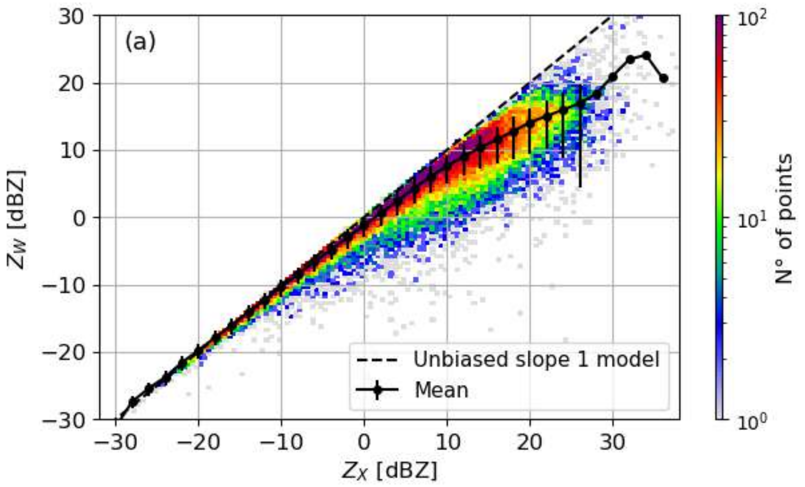

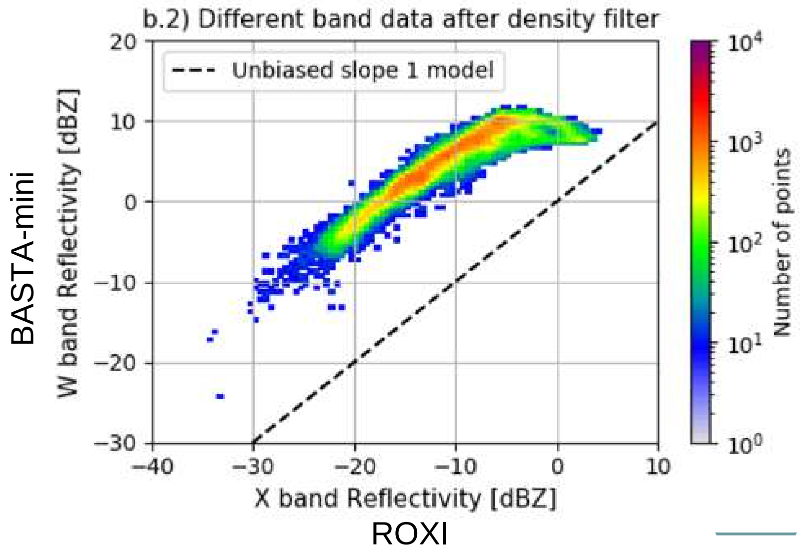

Data processing : Reflectivity range selection

- Reflectivity range selection
  - A correct comparison assumes a $y = 1 \cdot x + b$ model
    $$Z_r(r) = Z_u(r) + CC$$
  - Departure from the model is avoided by selecting comparable data pairs
  - Data selection is done using -45° degree lines
  - Criteria to select the appropriate range:
    - Selected data must have a slope as close as possible to 1
    - Minimization of the RMSE and maximization of R2 with respect to the slope 1 model
    - Minimization of discarded data. Max allowed data removal: 40%.

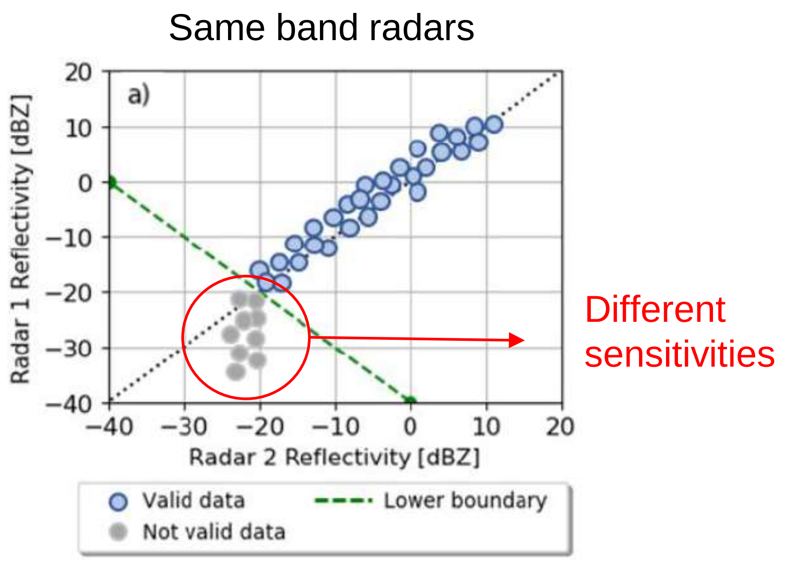

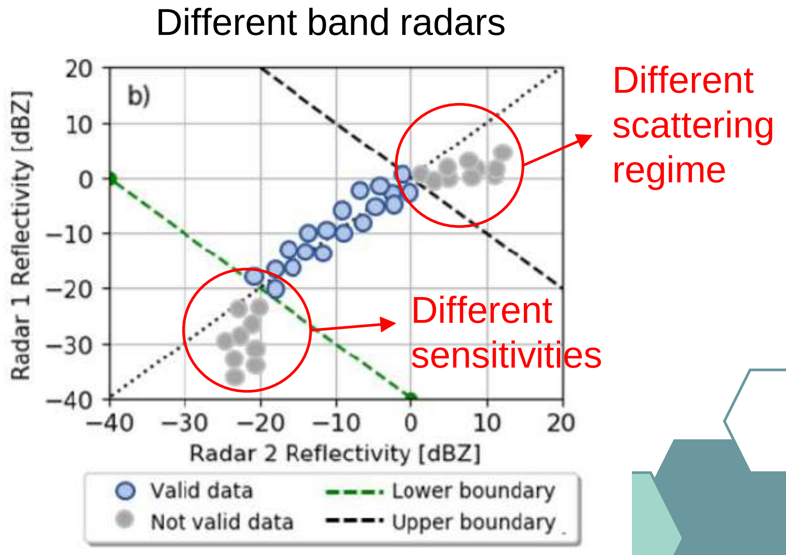

Correction coefficient estimation

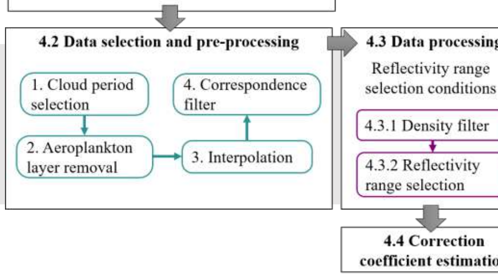

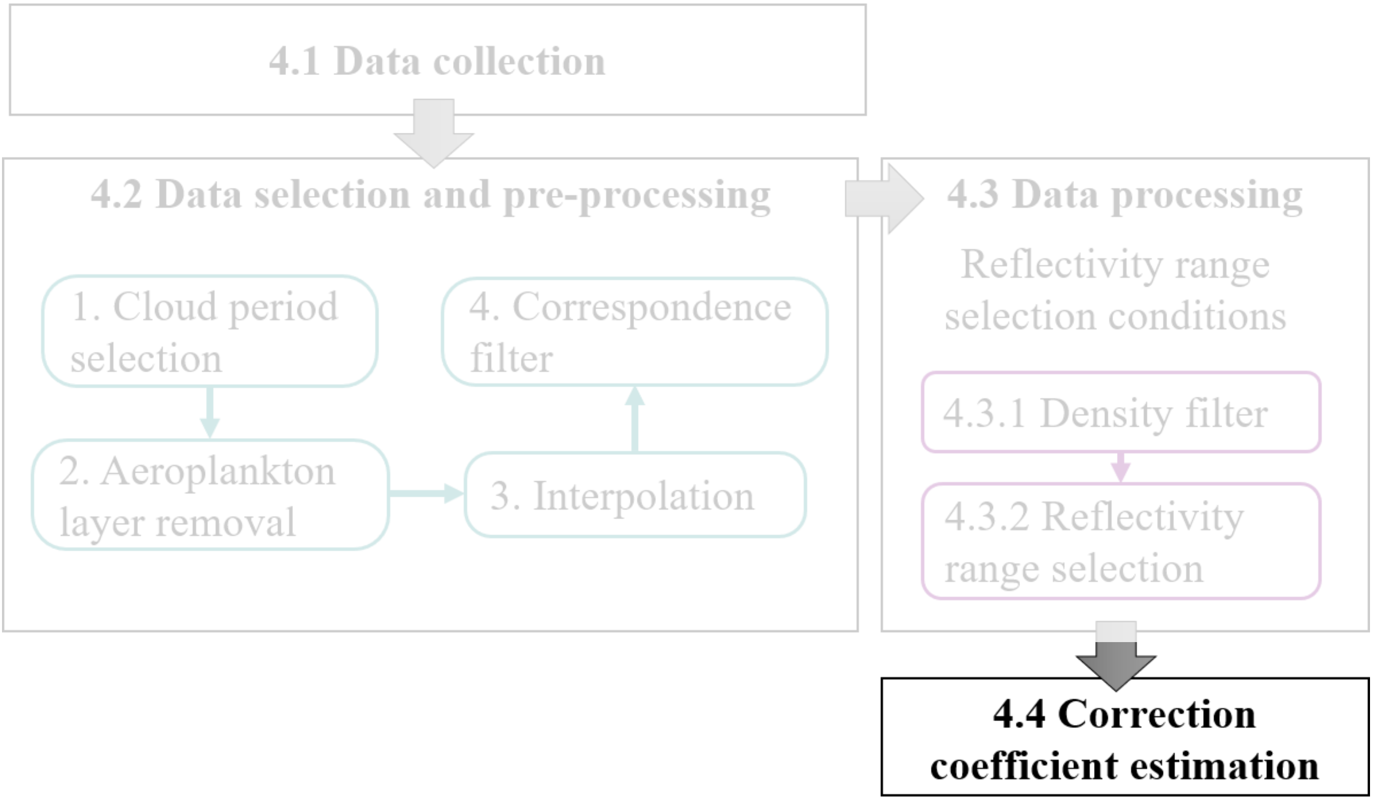

Correction coefficient estimation

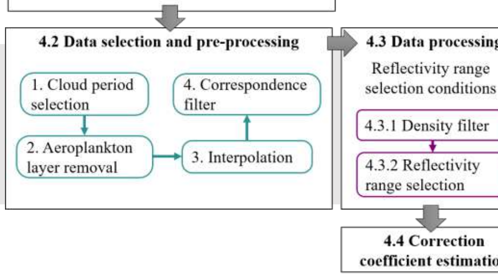

- CC is calculated fitting the slope 1 model

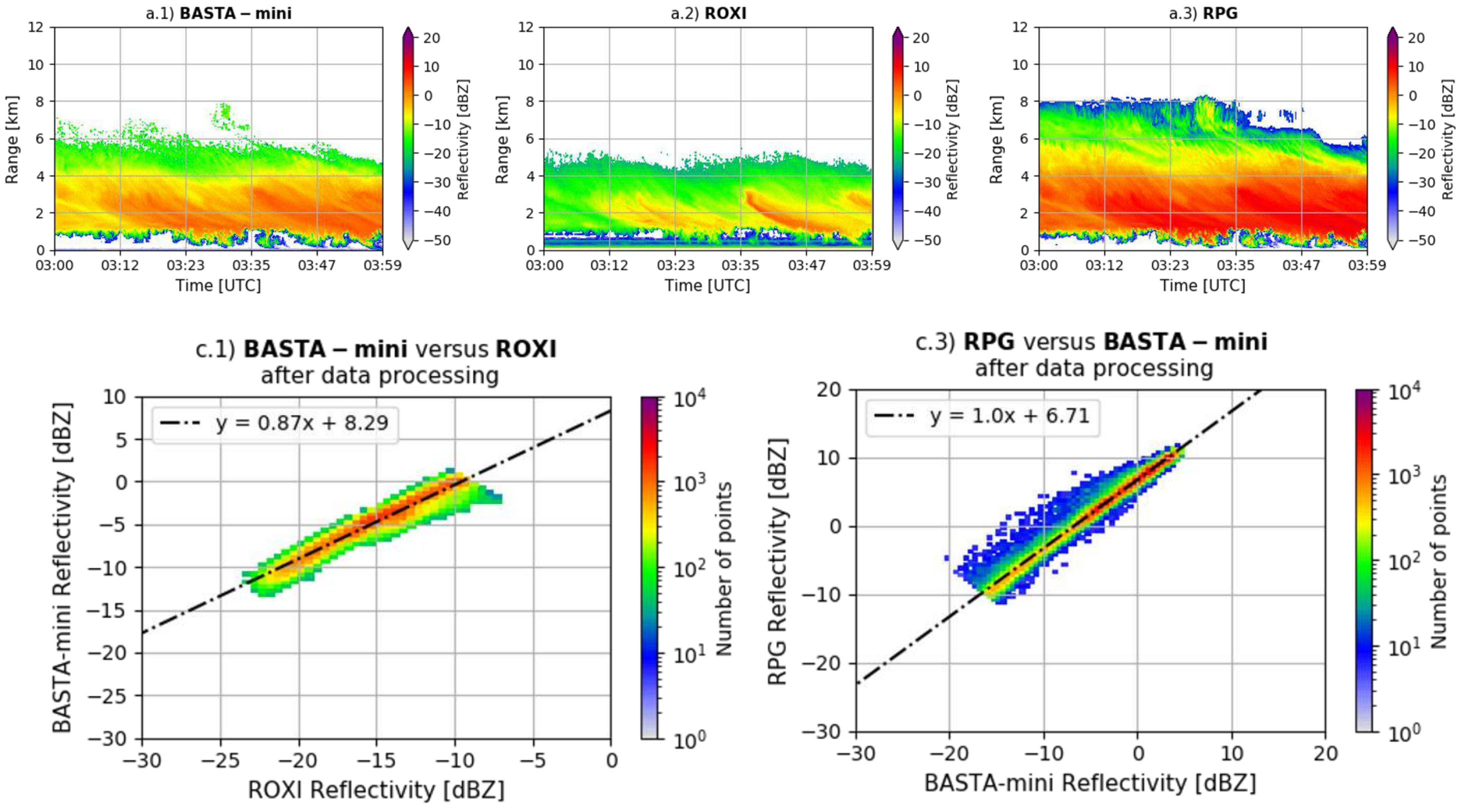

Radars compared	$CC[dB]$
$Z_{RPG} - Z_{BASTA_{mini}}$	6.7 ± 0.7 *
$Z_{BASTA_{mini}} - Z_{ROXI}$	10.3 ± 1.0

* BASTA had snow cover when sampling this cloud, absolute values are not the focus of this presentation

Correction coefficient estimation

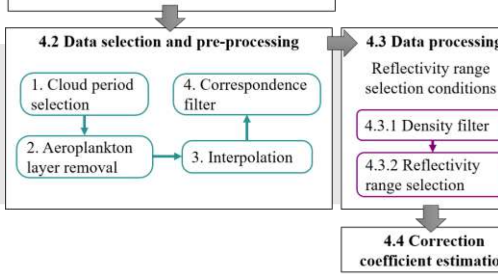

- Successive calibration using different clouds enables a reduction in uncertainty

Improvement of CC estimation as a function of the number of cloud periods analized
BASTA-Mini vs BASTA-mobile

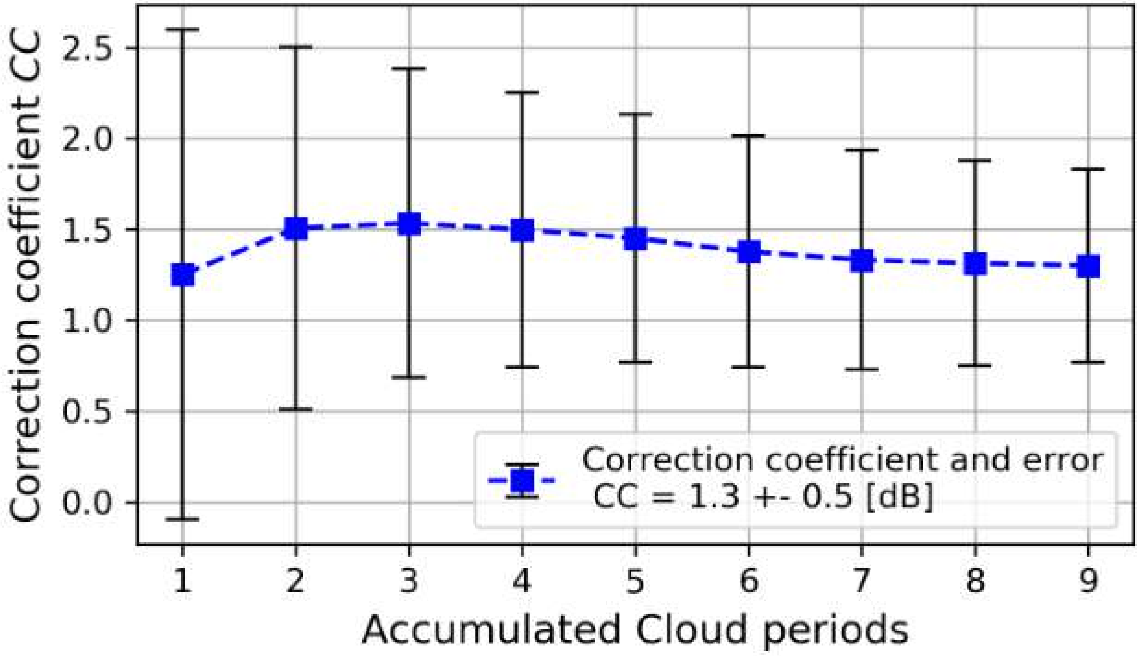

Method Validation

- The method is validated by closure, performing three cyclic calibration transfers between different band radars

Radars compared	$CC[dB]$
$Z_{RPG} - Z_{BASTA_{mini}}$	6.7 ±0.7
$Z_{BASTA_{mini}} - Z_{ROXI}$	10.3 ±1.0
$Z_{ROXI} - Z_{RPG}$	-16.7 ±1.2
R_{case2}	0.3 ±1.7

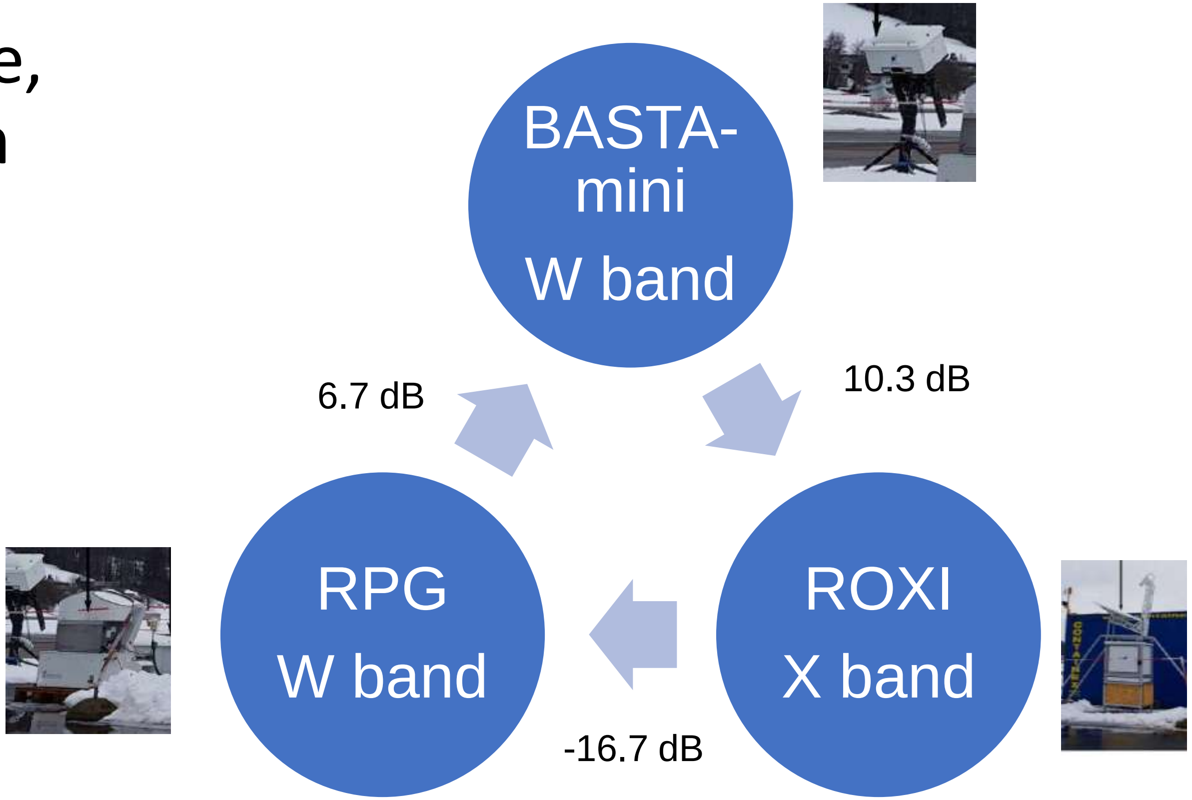

Residual of 0.3 dB after three successive calibration transfers

Cabauw calibration campaign

- Test of a 95 - 35 GHz calibration transfer using a dual frequency RPG radar
- Method tested with one experiment from the 2021 ACTRIS Cloud Radar calibration campaign carried out in Cabauw, The Netherlands

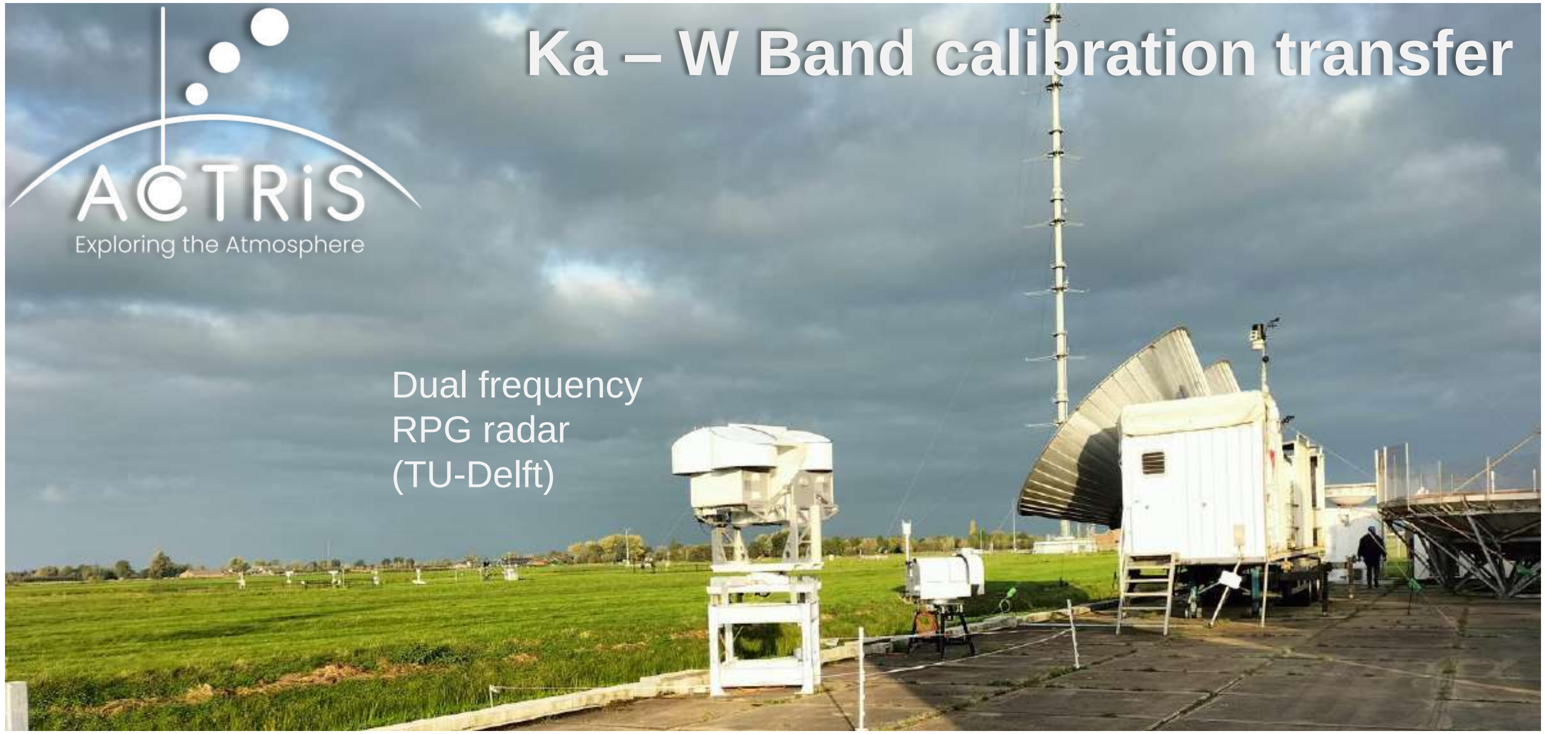

Cabauw calibration campaign

- Reflectivity retrievals from this radar have a relative bias <0.2 dB between both frequency bands

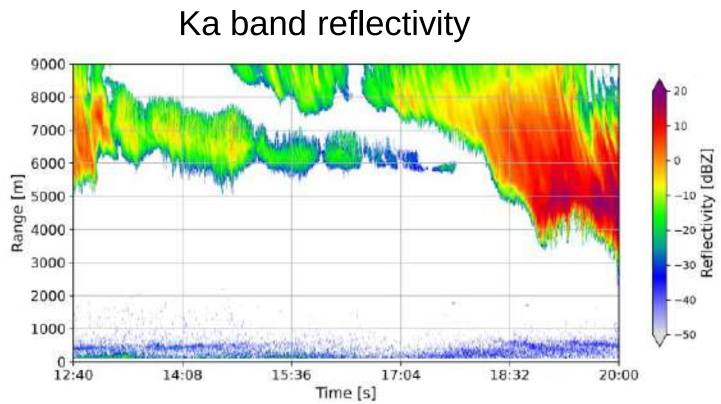

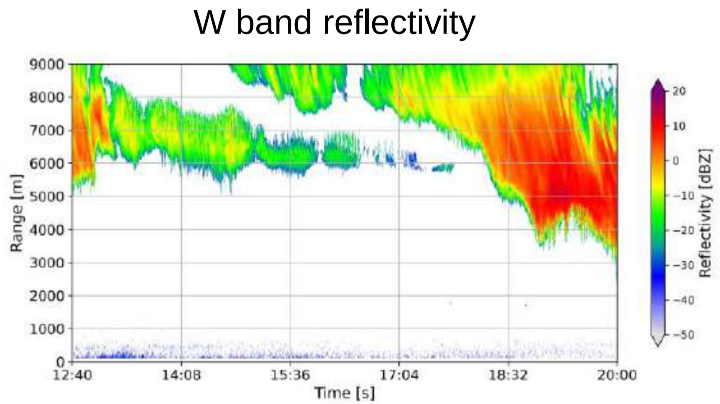

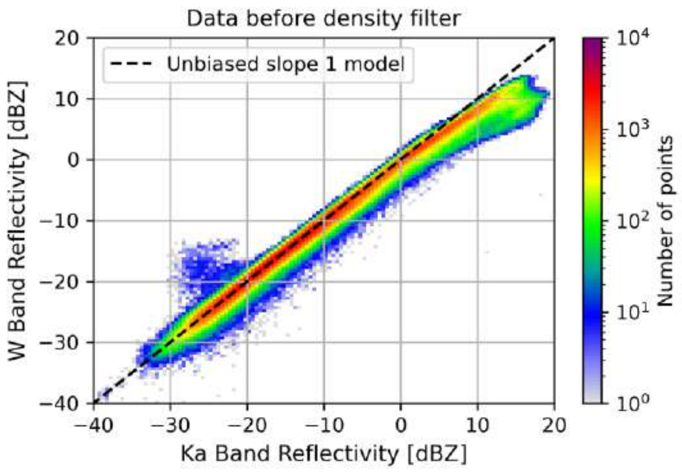

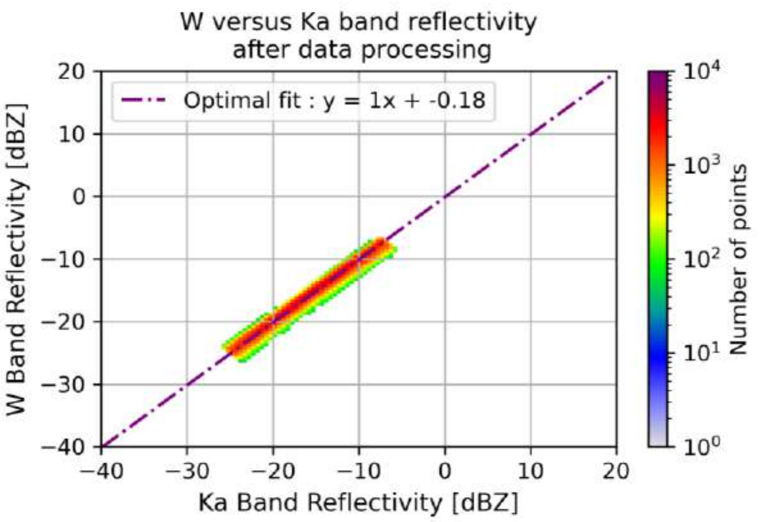

Cabauw calibration campaign

- Strong rain introduces a relative bias between reflectivity values for each frequency. Possible sources:
  - Differences in attenuation, specially due to liquid particles
  - Impact of wind direction (radomes may be suject to different amounts of rainfall accumulation)
- This method can be used to detect and quantify relative reflectivity biases

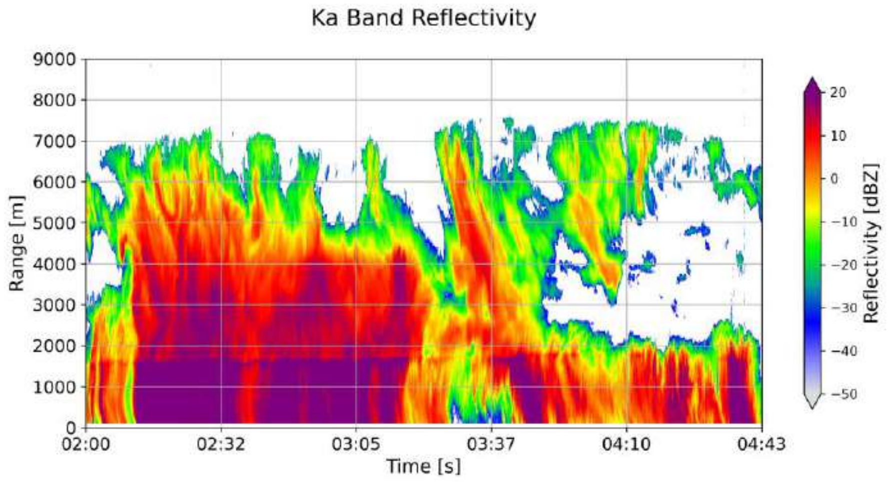

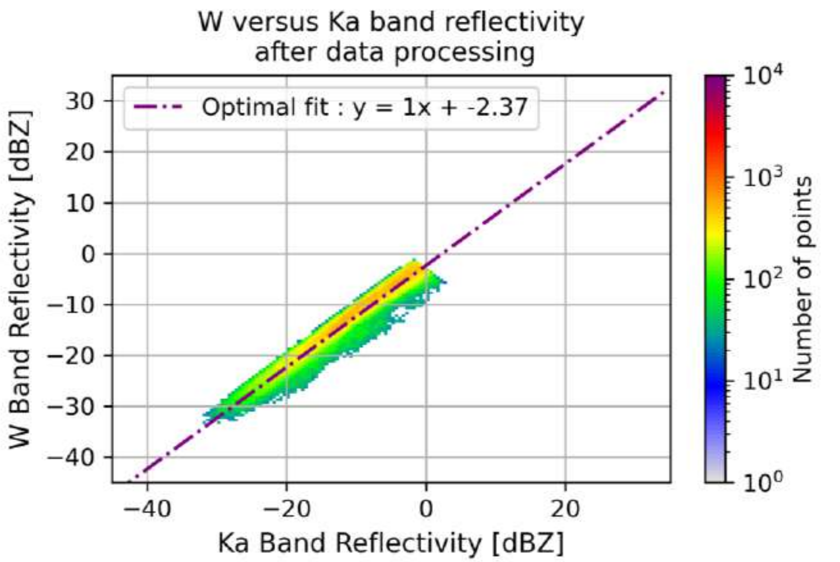

Conclusions

- A replicable calibration transfer method is developed
- This method enables calibration between same and different band radars based on simultaneous observation of ice cloud profiles
- Transfer uncertainties can reach values under 1 dB if enough repetitions are performed
- The method is validated by closure and has been tested at the X, W and Ka bands

Perspectives

- SIRTA will be equiped with reference W and X band radars
- The use of the presented methodology would enable calibration transfer for radar operating in the 10 to 95 GHz range
- To simplify the execution of this procedure, automatic ice cloud detection will be implemented taking advantage of the multiple instrumentation available at SIRTA